



Gene expression and metabolic activity of *Streptococcus mutans* during exposure to dietary carbohydrates glucose, sucrose, lactose, and xylitol

Veronika Jurakova¹  | Veronika Farková¹ | Jiri Kucera¹ | Katerina Dadakova¹ |
 Martina Zapletalova¹ | Katerina Paskova¹ | Roman Reminek² | Zdenek Glatz¹ |
 Lydie Izakovicova Holla^{3,4} | Filip Ruzicka⁵ | Jan Lochman¹  |
 Petra Borilova Linhartova^{3,4,6,7}

¹Department of Biochemistry, Faculty of Science, Masaryk University, Brno, Czech Republic

²Institute of Analytical Chemistry of the CAS, Brno, Czech Republic

³Clinic of Stomatology, Institution Shared with St. Anne's University Hospital, Faculty of Medicine, Masaryk University, Brno, Czech Republic

⁴Department of Pathophysiology, Faculty of Medicine, Masaryk University, Brno, Czech Republic

⁵Institute for Microbiology, Faculty of Medicine, Masaryk University and St. Anne's University Hospital, Brno, Czech Republic

⁶RECETOX, Faculty of Science, Masaryk University, Brno, Czech Republic

⁷Clinic of Maxillofacial Surgery, Institution Shared with University Hospital Brno, Faculty of Medicine, Masaryk University, Brno, Czech Republic

Correspondence

Petra Borilova Linhartova, Clinic of Stomatology, Institution Shared with St. Anne's University Hospital, Faculty of Medicine, Masaryk University, Pekarska 664/53, 602 00 Brno, Czech Republic.
 Email: petra.linhartova@recetox.muni.cz

Jan Lochman, Department of Biochemistry, Faculty of Science, Masaryk University, Kotlarska 2, 611 37 Brno, Czech Republic.
 Email: jlochman@sci.muni.cz

Jan Lochman and Petra Borilova Linhartova share the last authorship.

Funding information

Ministry of Health of the Czech Republic, Grant/Award Numbers: NV17-30439A, NU20-08-00205; Institutional Research Fund of Masaryk University, Grant/Award Number:

Abstract

Recent RNA sequencing studies have given us a deeper insight into the cariogenic impact of carbohydrate sources in the bacterium *Streptococcus mutans*, the principal microbial agent in dental caries etiopathogenesis. The process of dental caries development is facilitated by the ability of this bacterium to ferment some carbohydrates into organic acids contributing to a pH decrease in the oral cavity and the demineralization of the hard tissues of the tooth. Furthermore, in dental caries progression, biofilm formation, which starts and ends with free planktonic cells, plays an important role and has several unique properties called virulence factors. The most cariogenic carbohydrate is sucrose, an easily metabolizable source of energy that induces the acidification and synthesis of glucans, forming typical bacterial cell clumps. We used multifaceted methodological approaches to compare the transcriptomic and metabolomic profiles of *S. mutans* growing in planktonic culture on preferred and nonpreferred carbohydrates and in fasting conditions. *Streptococcus mutans* in a planktonic culture with

Abbreviations: ATP, adenosine triphosphate; BHI, brain–heart infusion; CLSM, confocal laser scanning microscopy; CRE, cAMP response element; CSP, competence-stimulating peptide; DEG, differentially expressed gene; EPS, extra polymeric substance; GFT, glucosyltransferase; IPS, intracellular polysaccharide; OD, optical density; PBS, phosphate-buffered saline; PCA, principal component analysis; PTS, phosphotransferase system; RGP, rhamnose–glucose polysaccharide; RNA-Seq, RNA sequencing; RT-PCR, real-time polymerase chain reaction; TCA, tricarboxylic acid; TCS, two-component systems; TSB, tryptone soya broth; VFA, volatile fatty acid.

This is an open access article under the terms of the [Creative Commons Attribution-NonCommercial](https://creativecommons.org/licenses/by-nc/4.0/) License, which permits use, distribution and reproduction in any medium, provided the original work is properly cited and is not used for commercial purposes.

© 2023 The Authors. *Molecular Oral Microbiology* published by John Wiley & Sons Ltd.

MUNI/A/1492/2021; European Union's Horizon 2020 Research and Innovation Programme, Grant/Award Number: 857560; MEYS CR, Research Infrastructure RECETOX RI, Grant/Award Number: LM2018121; MEYS CR, CETOCOEN EXCELLENCE, Grant/Award Number: CZ.02.1.01/0.0/0.0/17_043/0009632; Czech-BioImaging large RI project, Grant/Award Number: LM2023050

lactose produced the same pH drop as glucose and sucrose. By contrast, xylitol and lactose showed high effectiveness in regulating intracellular polysaccharide metabolism, cell wall structure, and overall virulence involved in the initial phase of biofilm formation and structure but with an opposite pattern compared with sucrose and glucose. Our results confirmed the recent findings that xylitol and lactose play a vital role in biofilm structure. However, they do not reduce its formation, which is related to the creation of a cariogenic environment.

KEYWORDS

cariogenic carbohydrates, cell wall, metabolome, RNA-Seq, *Streptococcus mutans*, transcriptome

1 | INTRODUCTION

The bacterium *Streptococcus mutans* is a substantial part of the human oral microbiota, and due to its virulent properties, it is considered the main etiological agent of dental caries. *Streptococcus mutans* belongs to lactic acid bacteria, which ferments carbohydrates (hexoses) mostly by homolactic fermentation. Based on glycolysis, this is also referred to as the Embden–Meyerhoff pathway. This pathway reduces pyruvate with NAD⁺-dependent lactate dehydrogenase in the final product, lactic acid (Pessione, 2012; Salminen et al., 2004).

The ability of this bacterium to ferment some carbohydrates into organic acids, such as lactic acid, contributes to the pH decrease in the oral cavity. Low pH values in the environment lead to the demineralization of the hard tissues, especially enamel, thus beginning the process of dental caries development. Although dental caries is usually not a life-threatening disease, its prevalence is high across the population, and its cure is considerably expensive.

The cariogenicity of *S. mutans* is conditioned by several unique properties called virulence factors (Balakrishnan et al., 2000). Adhesion, acidogenicity, and acid tolerance are considered the most important ones in addition to the ability to create intracellular polysaccharides (IPs) and produce bacteriocins. Each of these properties contributes to a change in the ecology of dental plaque and the subsequent dominance of *S. mutans* (Banas, 2004). Two processes are distinguished during the adhesion of *S. mutans* in dental plaque: reversible initial attachment and irreversible sucrose-dependent adhesion. The primary process of sucrose-dependent adhesion is the synthesis of glucans, polymers arising from dietary sucrose in the presence of glucosyltransferases (GTFs). Three genes, *gtfB*, *gtfC*, and *gtfD*, encode GTFs in *S. mutans*. Due to the synthesis of glucans and the ability to easily create hydrogen bonds, *S. mutans* forms typical bacterial cell clumps observed during cultivation (Balakrishnan et al., 2000; Banas, 2004; Zeng & Burne, 2013).

The acidogenicity of *S. mutans* is provided by organic acids. Lactic acid is produced the most, thereby contributing the most to the acidification of the environment. The acidogenicity of *S. mutans* is accompanied by the ability to tolerate low pH. Some strains can grow and retain metabolic activity even at a pH lower than 4.4, which usually inhibits bacterial growth (Banas, 2004). Acid tolerance is caused by a multitude of mechanisms working in concert—one of the cru-

cial is the membrane F₁F₀-ATPase, which helps to pump protons (H⁺) out of the cell. It is supported by the synthesis of glucans, which affect H⁺ diffusion and biofilm formation due to their physical characteristics (Ajdic et al., 2002). The production of IPs increases the virulence of the bacterium because the metabolism of these storage saccharides prolongs the exposure to organic acids when an external food source is no longer available (Islam et al., 2007). The production of bacteriocins, called mutacins in *S. mutans*, is also discussed as an important factor. Mutacins are small peptidic molecules that help to compete with other bacterial species (Merritt & Qi, 2012).

The most cariogenic carbohydrate is considered sucrose, an easily metabolizable source of energy (Zeng & Burne, 2013). Sucrose can be either cleaved outside the cell with extracellular enzymes GTF and fructosyltransferase or it has to be transported inside the cell (Colby & Russell, 1997). For this purpose, *S. mutans* utilize either primary active transport through a specific phosphotransferase system (PTS) or secondary active transport during carbohydrate translocation via the nonspecific or semispecific membrane permease (Peng et al., 2009). A PTS system catalyzes the simultaneous translocation and phosphorylation of mono- and disaccharides through several enzymatic reactions that transfer a phosphate group from phosphoenolpyruvate to a transported carbohydrate.

Dental biofilm plays a significant role in dental caries development and/or progression, and its formation is a complex, rapidly evolving process with several phases (Huang et al., 2011; Krzysciak et al., 2016). Although the cells are attached to the biofilm, the whole biofilm life cycle starts and ends with free planktonic cells. Several studies on biofilm-detached cells have already been published (Assaf et al., 2015; Duarte et al., 2008; Falsetta et al., 2014; Koo et al., 2010). Still, there is a gap in the knowledge of the properties of planktonic phase cells (Liu et al., 2013). The virulence and dental biofilm formation of *S. mutans*, considered the most cariogenic oral streptococci, largely rely on the availability of carbohydrates for energy and survival. Thus, the descriptions of the processes activated after sensing the sources of particular carbohydrates are of great importance.

This study aimed to perform RNA sequencing (RNA-Seq) analysis of *S. mutans* grown in a medium supplemented with various fermentable and nonfermentable carbohydrates to show the reprogramming of the *S. mutans* transcriptome.

2 | MATERIAL AND METHODS

2.1 | Bacterial strain and growth conditions

Streptococcus mutans (strain UA159) was cultured in brain–heart infusion (BHI) broth (Sigma–Aldrich) under an atmosphere of 95% air and 5% CO₂ at 37°C with shaking. The overnight culture was then centrifuged at 6000 × *g* for 10 min, and the pellet was washed once with tryptone soya broth (TSB) without glucose (Sigma–Aldrich) and resuspended in the same medium. As prepared, 4% (v/v) of the culture was then inoculated into a fresh TSB medium supplemented with 0.5% (w/v) carbohydrate (sucrose, glucose, lactose, xylitol, or none). The 30 mL of cultures were then cultivated with shaking in closed 50-mL TubeSpin® Bioreactor 50 tubes (TPP) at 37°C in a CO₂ incubator (5% CO₂ atmosphere).

For transcriptomic analysis, *S. mutans* cultures were harvested in the mid-exponential phase (after 6 h). High-yield cultures grown on sucrose, glucose, and lactose were diluted twofold with phosphate-buffered saline (PBS), and a total of 5 mL was used. Low-yield cultures incubated in the absence of carbohydrates or the presence of xylitol were not diluted, and a total of 10 mL was used. The cultures were centrifuged at 6000 × *g* and 4°C for 10 min. The cell pellets were washed twice with PBS buffer and immediately proceeded to RNA isolation.

For metabolomic analysis, *S. mutans* cultures were harvested in the mid-exponential phase (after 4 h). The cultures were centrifuged at 6000 × *g* for 10 min at 4°C. The supernatants were separated, while the pellet was stored at –80°C until further processing. Furthermore, the samples were collected every hour for volatile fatty acid (VFA) analysis and every 2 h for DNA isolation. Cell growth was measured spectrophotometrically at 600 nm. The pH values were determined using a pHTestr 10 BNC (Eutech Instruments) and an Orion™ Economy Series pH combination electrode (Thermo Fisher Scientific).

2.2 | Quantitative real-time PCR

Streptococcus mutans was quantified by real-time polymerase chain reaction (RT-PCR) amplification of the *ilvB* gene. To isolate the DNA, the culture samples were centrifuged at 6000 × *g* for 10 min at 4°C. The pellets were washed once with 500 μL of nuclease-free water and then resuspended in another 500 μL of nuclease-free water. Mechanical homogenization was performed using a 2-mL Potter–Elvehjem homogenizer. Subsequently, the samples were heated to 90°C for 10 min and centrifuged at 10,000 × *g* for 10 min. The RT-PCR included 2 μL fivefold diluted sample, 0.06 μL 50 μM *ilvB* reverse and forward primer mixture (sequences are listed in Table S1), 5 μL 2× LunaMix (New England Biolabs, USA), and 3 μL nuclease-free water. The RT-PCRs were performed in the LightCycler® 480 system (Roche) using a program consisting of an initial denaturation at 95°C for 2.5 min, 40 cycles of denaturation at 95°C for 10 s, and annealing/extension at 40°C for 40 s. After each RT-PCR run, melting curves were constructed with the following parameters: one cycle of 95°C for 5 s and 60°C for 30 s followed by a temperature ramping up to 95°C in 0.3°C steps.

2.3 | VFA analysis

As carbohydrate fermentation leads to a mixture of organic acids, including VFAs, these acids were quantified during the growth of *S. mutans* with various carbohydrates. The samples were centrifuged at 4000 × *g* for 5 min, and 720 μL of supernatant was mixed with 300 μL 10% (v/v) formic acid and 480 μL 100 mM periodic acid. The mixture was heated at 100°C for 60 min in a tube with a screw cap. The mixture was cooled first for 5 min at room temperature and then for 20 min in a refrigerator. Afterward, the mixture was vortexed for 30 s, and 250 μL of the sample was filtrated through a Durapore membrane filter with a pore size of 0.45 μm (Merck) (Darwin et al., 2018). In the case of formic acid analysis, the samples were centrifuged at 4000 × *g* for 5 min, and 100 μL of supernatant was mixed with 900 μL of ultrapure miliQ water and filtrated through a Durapore membrane filter with a pore size of 0.45 μm (Merck).

Gas chromatography analysis of the VFAs was performed using an Agilent 8860 (Agilent Technologies) with flame ionization detection. Formic acid, acetic acid, propionic acid, butyric acid and lactic acid were separated using a DB-WAX capillary column (30 m × 0.32 mm × 0.25 μm) at a flow rate of 2 mL/min, split 10:1 at the inlet (helium was used as carrier gas). The injection volume was set up at 1 μL and performed with a 10-μL syringe (Agilent Technologies), and the run time was programmed at 13.5 min. The oven temperature was programmed as follows: an initial temperature of 50°C (5 min) and a ramp rate of 20°C/min to 180°C (2 min). The injector and detector temperatures were set at 250°C.

2.4 | Analysis of carbohydrate composition of clumps

To generate clumps, *S. mutans* was cultivated in a TSB medium with sucrose for 6 h. The culture was then centrifuged at 4000 × *g* for 5 min, then 1 mL of lysis buffer (50 mM TRIS, 150 mM NaCl, 1% Triton, pH 7.5) was added to the pelleted clumps and homogenized by needle sonication (180 × 0.1 s pulses at 15 W; HD 2200, Bandelin). The pellets were washed three times with 500 μL of 10 mM ammonium acetate (pH 5.6) and resuspended in 100 μL of the same.

Carbohydrates were determined in the complex mixtures after the acidic hydrolysis of carbohydrate polymers according to the method described by Rühmann et al. (2014). To 15 μL of the sample, 5 μL of 10 mM ammonium acetate (pH 5.6) and 20 μL of 4 M trifluoroacetic acid were added and incubated at 121°C for 90 min. The pH value was adjusted to 8 with 3.2% ammonium hydroxide. Consequently, 25 μL of the sample or carbohydrate standards (50 mg/L) was mixed with 75 μL of derivatization reagent (0.1 M 1-phenyl-3-methyl-5-pyrazolone [PMP] in methanol and 0.4% ammonium hydroxide in ratio 2:1). The mixture was incubated at 70°C for 100 min and then cooled to 20°C. Aliquots of 20 μL were transferred to a new tube and mixed with 130 μL of 19 mM acetic acid. The mixture was filtrated through a 0.45-μm pore size Durapore membrane filtrate (Merck) by centrifugation at 2500 × *g* for 5 min. HPLC analysis of the carbohydrates was performed

using an Agilent 1200 Infinity Series (Agilent Technologies) with a diode array detector (210 and 245 nm). The carbohydrates were separated using an EC 100/2 Nucleodur C18 Gravity-SBS column (1.8 μm particle size, 110 \AA , 2 mm \times 100 mm; Macherey-Nagel) tempered to 50°C at a flow rate of 0.6 mL/min with the following LC gradient program where mobile phase A was 15% (v/v) acetonitrile in 5 mM ammonium acetate (pH 5.6), and mobile phase B was acetonitrile: the proportion of mobile phase B was increased from the initial value of 6% to 10% over 5 min, raised to 23% over 1 min, then further raised to 45% over 0.3 min, held at 45% for 2 min, and returned within 0.2 min to the starting conditions for 1.5 min (Rühmann et al., 2014). The data were analyzed using the ChemStation software (Agilent Technologies).

2.5 | RNA sequencing

For RNA isolation, the washed pellets were homogenized using an MM301 mixer mill (Retsch GmbH) with 3-mm stainless steel grinding beads for 1 min at a frequency of 20 Hz. The total RNA was isolated with a Tri Reagent[®] (Merck) and treated with a RapidOut DNA Removal Kit (Thermo Fisher Scientific) to remove contaminating DNA. The quality and quantity of the RNA were assessed with a Qubit 4 fluorometer (Thermo Fisher Scientific) and fragment analyzer (Agilent Technologies).

The cDNA libraries were constructed using the ScriptSeq[™] Complete Kit (Illumina) for bacteria, including Ribo-Zero[™] technology for ribosomal RNA removal and the ScriptSeq v2 RNA-Seq Library Preparation Kit. The quality and quantity of the cDNA libraries were assessed with a Qubit 4 fluorometer (Thermo Fisher Scientific) and fragment analyzer (Agilent Technologies). Finally, the cDNA libraries were diluted to the final concentration of 10 nM. Sequencing was performed on the Illumina[®] NextSeq[®] platform with the NextSeq 500/550 High Output Kit v2.5 (150 cycles), which generated 75 bp pair-end reads. Transcriptomic data processing was performed as described previously (Kucera et al., 2020) using the genome *S. mutans* strain UA159 (AE014133).

2.6 | Metabolomic analysis

Metabolite extraction was performed as previously described (Depke et al., 2017). Briefly, the thawed cell pellets were resuspended in 500 μL 80% (v/v) methanol containing 0.1 mg/L trimethoprim, 0.1 mg/L nor-triptyline, and 0.3 mg/L glipizide as internal standards. Cell disruption was achieved by vortexing for 1 min followed by sonication in an ice-cold sonic bath (Branson 5510 Ultrasonic bath; Marshall Scientific) for 15 min. Cell debris was removed by centrifugation at 11,000 $\times g$ for 20 min at 4°C. Then, 400 μL of each extract was dried in a centrifugal evaporator (SpeedVac SPD111V; Thermo Fisher Scientific) at 35°C and a full vacuum until complete dryness. The samples were reconstituted in 40 μL 5% (v/v) methanol with 0.01% (v/v) acetic acid containing 1 mg/L of caffeine and 8 mg/L of naproxen as internal standards (Depke

et al., 2020). The samples were filtered by centrifugal filters (0.2 μm pore size, hydrophilic PTFE; Merck) at 8000 $\times g$ for 5 min and analyzed using the 6545 LC/Q-TOF system (Agilent Technologies). The analytes were separated using an EclipsePlus C18 (1.8 μm particle size, 95 \AA , 2.1 mm \times 100 mm; Agilent Technologies) reverse-phase column at a flow rate of 0.3 mL/min with the following LC gradient program where mobile phase A was 0.01% acetic acid in water, and mobile phase B was methanol: the proportion of mobile phase B was increased from the initial value of 5% to 20% over 10 min, raised to 100% between 10 and 20 min, held at 100% for 10 min, and decreased to 5% for 10 min for equilibration. An electrospray ion source was used under the following conditions: acquisition mode, 100–1700 m/z ; gas temperature, 300°C; gas flow, 8 L/min; negative ion polarity; capillary voltage, 4000 V; and fragmentor voltage, 150 V. Metabolites were detected by Q-TOF, processed in the MassHunter Profinder software (Agilent Technologies), and putatively identified by comparing the obtained mass spectra with the database (Metlin, The Scripps Research Institute [metlin.scripps.edu]). For identification, iterative MS/MS data acquisition was used. The alignment of the chromatograms was performed based on the peaks of the internal standards.

2.7 | Quantification of biofilm biomass using crystal violet

Saliva samples, later used for disc coating, were collected from four healthy volunteers, centrifuged at 10,000 $\times g$ for 10 min at 4°C, and sterilized using a 0.22- μm Millex GS Filter Unit (Merck Millipore). Wells of 96-well polystyrene plate were coated with 40 μL human saliva for 1 h at 4°C. After that, wells were washed two times with 100 μL 1 \times PBS. The saliva-coated plate with 180 μL of TSB medium without carbohydrates or containing 0.5% concentrations of glucose, sucrose, lactose, or xylitol was inoculated with 20 μL of overnight *S. mutans* culture grown in BHI medium at 37°C in 95% air/5% CO₂. Consequently, the plate was incubated for 24 h at 37°C in 95% air/5% CO₂. Afterward, the generated biofilms were washed carefully twice using 200 μL of saline solution. The biofilms were stained using 0.1% crystal violet (Merck) solution similarly as described previously (Assaf et al., 2015). Following 20 min of incubation, the crystal violet was washed twice with saline and the stained biofilms were dried. Next, 33% acetic acid was added to elute the crystal violet for 30 min while shaking at room temperature. The extract was placed in a new 96-well plate and optical density (OD) at 600 nm was measured using an ELx808 BioTek plate reader (BioTek Instruments GmbH).

2.8 | Measurement of biofilm matrix

Saliva samples, later used for disc coating, were collected from four healthy volunteers, centrifuged at 10,000 $\times g$ for 10 min at 4°C, and sterilized using a 0.22- μm Millex GS Filter Unit (Merck Millipore). Hydroxyapatite discs ($d = 1.3$ cm; in a 24-well plate) were coated with 500 μL human saliva for 1 h at 4°C. After that, discs were washed two

times with 1000 μL 1 \times PBS. Such pre-prepared discs were inoculated with the 4% (v/v) culture in the TSB medium supplemented with 0.5% (w/v) carbohydrate (sucrose, glucose, lactose, xylitol, or none) and cultivated under an atmosphere of 95% air and 5% CO_2 at 37°C for 24 h. The density and architecture of the extra polymeric substance (EPS), referred to as extracellular matrix, was determined by staining hydroxyapatite discs with cell-permeant nuclear acid counterstain Hoechst 33342 (Thermo Fisher Scientific) that emits blue fluorescence when bound to dsDNA and FilmTracer Sypro Ruby biofilm matrix stain (Thermo Fisher Scientific). Biofilms on hydroxyapatite discs in 12-well plates were rinsed with PBS and stained for 30 min at room temperature with 10 $\mu\text{g}/\text{mL}$ Hoechst 33342 in PBS or 1 mL of FilmTracer™ SYPRO™ Ruby Biofilm Matrix Stain (Thermo Fisher Scientific). The biofilms were then rinsed twice with PBS. The biofilms on hydroxyapatite discs were analyzed by a confocal laser scanning microscopy (CLSM) using an LSM880 (Carl Zeiss Microscopy, GmbH) equipped with an argon laser (458 nm). The confocal images were obtained using a Plan-Apochromat 100 \times /1.46 Oil DIC M27 Elyra immersion objective. Serial optical sections were recorded at 3.16 μm in the z-direction throughout the biofilm when the image frame was 792 \times 792 pixels in size.

2.9 | Statistical analysis

In the case of transcriptomic analysis, R package DESeq2 (Love et al., 2014) was used to pinpoint differentially expressed genes (DEGs) between TSB and individual carbohydrates and xylitol. The cutoffs for designating a gene as differentially expressed were a change in transcript levels of at least 1.5-fold and an adjusted *p*-value of less than 0.05 (Table S2; Figure S1). Next, we applied principal component analysis (PCA) to represent the transcriptomic similarities between TSB and individual carbohydrates visually.

In the case of metabolomic analysis, differences in the peak areas were assessed using a one-way analysis of variance with Benjamini-Hochberg correction in the Mass Profiler Professional 15.0 software (Agilent Technologies). The Tukey HSD test was used as a post hoc test. The *p*-value cutoff for significant results was set to 0.001 and the fold-change value to 10. The metabolic differences between samples were visualized using PCA.

3 | RESULTS

3.1 | Growth of *S. mutans* in the presence of glucose, sucrose, lactose, and xylitol

To characterize the effects of various carbohydrates on planktonic *S. mutans* cells, the growth kinetic parameters (OD, pH) and product concentrations (VFAs) were monitored (Figure 1a,c). As *S. mutans* generated large bacterial clumps in the medium with sucrose, as observed previously (Staat et al., 1980), bacterial growth could not be monitored by OD. Therefore, the growth was determined by quantifying the *ilvB* gene from the isolated DNA using the previously established

qPCR method (Lochman et al., 2019) (Figure 1a). The growth rates in the media containing glucose, lactose, and sucrose were considerably higher compared with xylitol. We observed a minimal growth rate similar to the control culture without carbohydrates in the case of xylitol (Figure 1a). Furthermore, the growth rates of the cultures in the media with the individual carbohydrates corresponded with a decrease in pH during the first 6 h of cultivation (Figure 1c).

The analysis of the VFAs showed that although propionic and butyric acid levels were relatively low and unchanged over time, the relationship corresponding to different carbohydrate metabolisms in lactic, formic, and acetic acids was observed (Figure 1b-f). Formic acid production was observed under mostly anaerobic conditions in closed culture tubes with limited aeration, as the pyruvate formate-lyase responsible for its production is an oxygen-sensitive enzyme. In *S. mutans* cultured with glucose and lactose, acetic and formic acid levels increased during the first 6 h to final concentrations of approximately 2.3 and 3.5 mM, respectively (Figure 1c,e). In *S. mutans* cultured with sucrose, an average increase in acetic and formic acids was observed during the first 6 h, ending with final concentrations of about 1.6 and 2.3 mM, respectively (Figure 1d). Moreover, in the presence of the sugar polyol xylitol, the increase was very modest and the final concentrations of acetic and formic acids were 1.16 and 1.84 mM, respectively (Figure 1f), indicating further growth inhibition compared to the control without carbohydrates. Lactic acid levels showed that *S. mutans* grown with the cariogenic carbohydrates (i.e., sucrose, glucose, and lactose) exhibited elevated production of this acid over time, unlike cultures grown with xylitol and without any carbohydrate (Figure 1b-f). It is important to note that the TSB medium used contained a nutritious plant peptone with a carbohydrate content of approximately 35%, including 25% of non-starch polysaccharides and 5% of the free sugar sucrose, which is preferred by *S. mutans* (Choct et al., 2010). Due to this fact, we monitored the level of sucrose in the TSB medium during the growth of *S. mutans*. The measured very low sucrose concentration (~0.015%) was metabolized by the growing culture within the first 3 h (Figure S1) and possibly represents the origin of the acetic acid produced by the culture at the beginning of cultivation.

3.2 | Transcriptomic changes of *S. mutans* induced by different carbohydrates

Total RNA was isolated either from *S. mutans* cultivated in the TSB medium without any carbohydrate or the 0.5% concentrations of the individual carbohydrates or xylitol and treated with the RiboZero kit (Illumina) to deplete the rRNAs, and cDNA libraries were then constructed and subjected to high-throughput sequencing (see Section 2). A total of 413,131,247 reads were produced from the 15 samples, with the median number of reads at 25,271,410 per sample (Supporting Information Data). The sequence reads of all samples were deposited in the NCBI Sequence Read Archive (SRA) as a study under the accession number GSE207392.

Individual replicates of the samples clustered separately (Figure 2a), indicating high levels of correlation and reproducibility among the

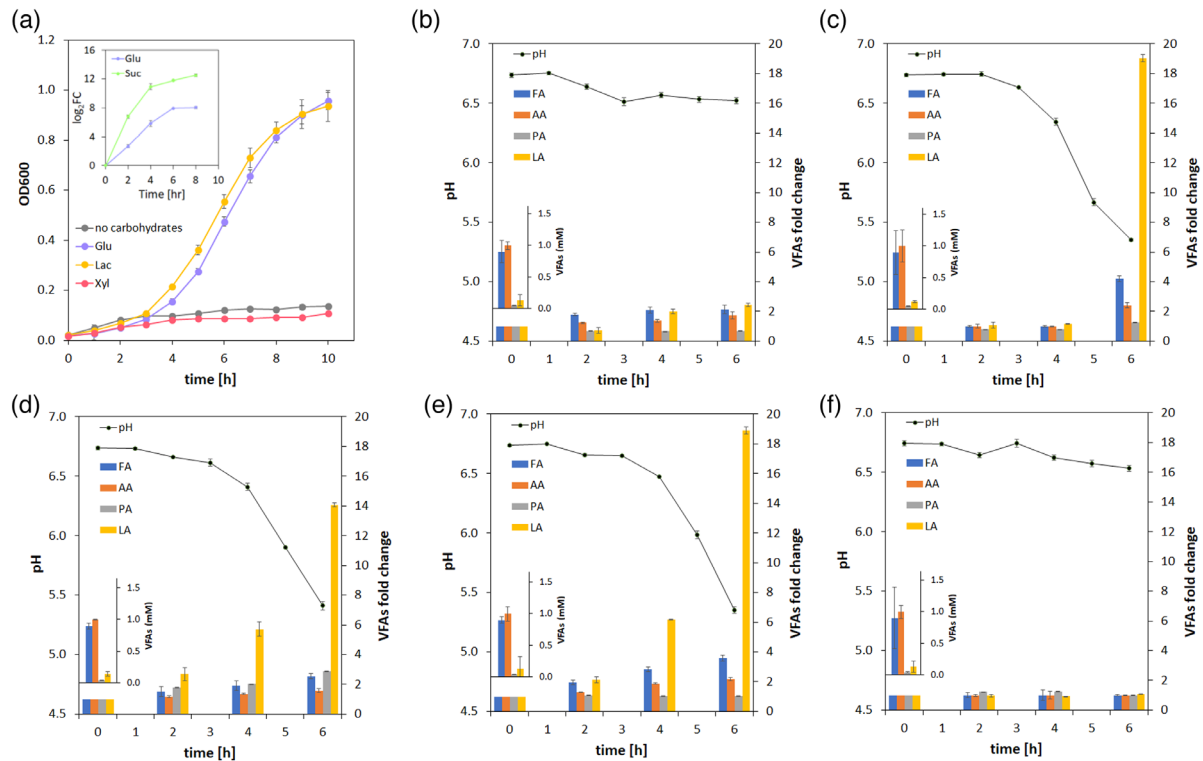


FIGURE 1 Growth characteristics of *Streptococcus mutans* on different carbohydrates and xylitol. (a) Growth curves of *S. mutans* ATCC 25175T. The growth curve of culture on sucrose measured by qPCR is shown in the inset. (B–F) pH drop and accumulation of formic acid, acetic acid, propionic acid, and lactate in the culture medium of *S. mutans* without carbohydrates (b) and media supplemented with 0.5% (w/v) of glucose (c), sucrose (d), lactose (e), and xylitol (f). The initial concentrations of individual volatile fatty acid (VFAs) are shown in insets. Accumulation of VFAs in the culture medium of *S. mutans* was measured by the Agilent 8860 gas chromatography with flame ionization detection. All cultivations were done in 50-mL TubeSpin® Bioreactors (TPP) on a rotary shaker (300 rpm) in a 5% CO₂ aerobic atmosphere at 37°C in tryptone soya broth (TSB) medium supplemented with 0.5% (w/v) carbohydrates. Error bars indicate the standard deviation of biological triplicates.

samples as well as distinctive transcriptome profiles from *S. mutans* in the presence or absence of carbohydrates. Noticeably, the glucose samples clustered differently from the samples cultivated in the presence of sucrose, lactose, or xylitol (Figure 2a). Overall, a substantial portion of the *S. mutans* transcriptome was significantly altered by the presence of the tested carbohydrates compared with the TSB (Figure 2c) when a significantly lower number of DEGs was observed in the samples cultivated in the presence of glucose. Interestingly, about 70% of up- and downregulated genes were shared between lactose and xylitol, but between sucrose and glucose, only 18% and 30% were shared for up- and downregulated genes, respectively (Figure 2b,d). However, the opposite regulation was observed between sucrose and lactose in 80% of genes and between sucrose and xylitol in 50% of genes (Figure 3a,b). Focusing on genes showing different expression levels, a subset of these results was confirmed using quantitative RT-PCR (Figure 3c).

3.2.1 | Expression levels of genes for PTS and carbohydrate metabolism

Most DEGs were included in carbohydrate metabolism (Figures 4 and 5a,b), mainly reflecting changes in PTS genes representing a major

carbohydrate transport system in oral streptococci related to glucose, sucrose, lactose, or xylitol uptake.

Glucose and sucrose, the activators of carbon catabolite repression, negatively affected major-glucose-PTS EII^{Man} (SMU_1877), which further directly negatively affected many PTS operons, including the genes for EII^{Lac} (SMU_1491-92, SMU_1498), EII^{Sorb/Mntl} (SMU_313), or EII^{Cel} (SMU_1598) (Zeng & Burne, 2008) (Figure 5a; Table s2). Furthermore, the transcripts for galactose metabolism *lacA-G* (SMU_1490-96) and *galkTE* (SMU_886-88) and pyruvate oxidation *adhA-D* (SMU_127-30) and *pf12* (SMU_493) were also downregulated (Figure 5b; Table s2). Compared with glucose, the growth of the cells with sucrose caused significantly more remarkable changes in the transcriptome (Figure 2b). In the case of PTS, there was upregulation of the EII^{Suc} gene *scrA* (SMU_1841) as a part of sucrose-specific PTS together with exoenzyme fructan hydrolase *fruA* (SMU_78), releasing fructose from sucrose, inducible PTS EII^{Fru} genes (SMU_870-72), and putative PTS EII^{Man} genes (SMU_1960-61c) (Figure 5a). Moreover, the genes for constitutive PTS EII^{Fru} (SMU_114-15) were downregulated (Figure 5a) as well as the multiple-sugar metabolism (*msm*) pathway genes (SMU_833-77), acetate kinase *ackA*, or *glg* operon (SMU_1535-39) responsible for bacterial glycogen synthesis (Figure 5b). Significant downregulation of phosphotransacetylase and acetate kinase corresponded to a lower accumulation of acetate in the medium during

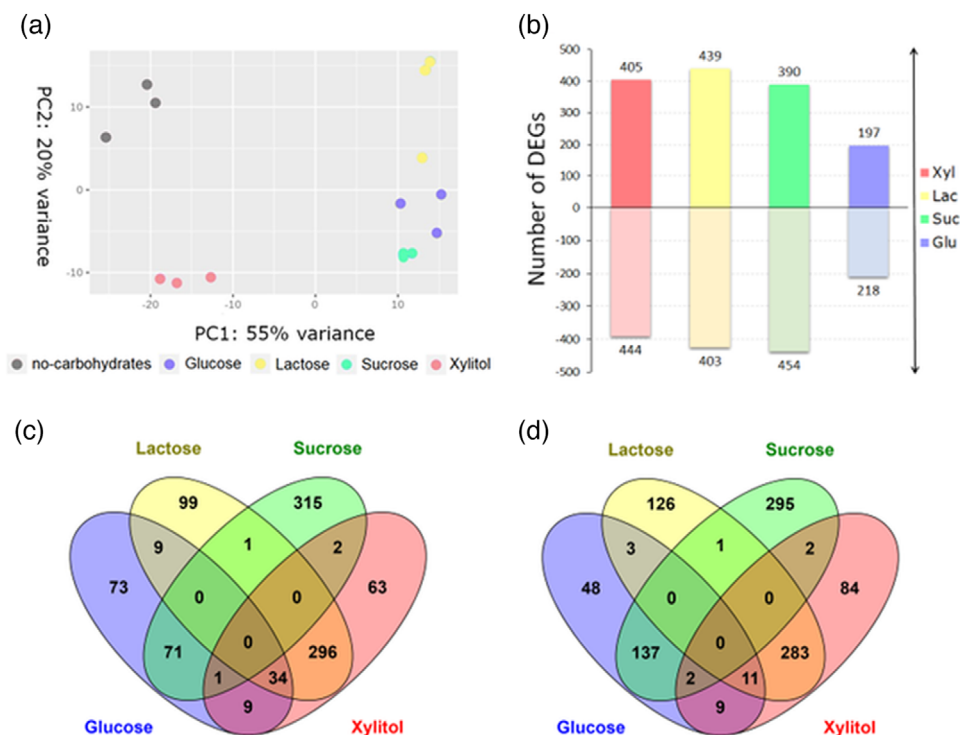


FIGURE 2 Overall transcriptomic changes associated with the cultivation of *Streptococcus mutans* on different carbohydrates and xylitol. (a) Principal component analysis (PCA) plot showing the clustering of samples, $p < 0.05$; gray—control tryptone soya broth (TSB), purple—xylitol, yellow—lactose, green—sucrose, and red—glucose. (b) Total number of genes differentially expressed during the cultivation of *S. mutans* on different carbohydrates (calculated as the ratio between the expression in 0.5% [w/v] carbohydrates and the TSB medium alone) at the exponential growth phase 6 h after inoculation. A > 1.5 -fold difference and $p_{\text{adj}} < 0.05$ were used as the cutoff. The number of genes in each category is shown. The Venn diagrams show the overlap between upregulated (c) and downregulated (d) genes in cells treated with different carbohydrates.

the cultivation of the cells with sucrose (Figures 1c and 5b). However, the Sec secretion pathway translocating virulence factors across the cytoplasmic membrane, ribosomal genes, and genes of the citric cycle (SMU_670-72), together with adenosine triphosphate (ATP) synthase involved in proton expulsion, were upregulated during the growth with sucrose (Figures 4a and 5b). The genes (SMU_1339-40, SMU_1341c, SMU_1342, SMU_1343c, and SMU_1345c) involved in the production of membrane vesicles, which are associated with biofilm formation (Wen et al., 2021), were upregulated in the presence of glucose.

By contrast, a vast number of carbohydrate acquisition PTS genes were downregulated in the glucose-growing cells, including major-glucose-PTS EII^{Man} (SMU_1877), which showed increased expression levels in the lactose-growing cells and cells cultured with xylitol (Figures 4 and 5a). Compared with lactose, there was no increase in the presence of xylitol, only in the PTS genes for sucrose (SMU_1840-41), fructose (SMU_113-16), and lactose (SMU_1491-92). Meanwhile, the genes for nigerose-specific (SMU101-03) and putative mannose-specific (SMU_1960-61c) PTS were upregulated only on xylitol (Figure 5A). With regard to carbohydrate metabolism, growing with lactose and xylitol resulted in almost opposite gene regulation (Figures 4 and 5b) compared with sucrose and glucose (Figure 5B; Table S1). There was activation of the *glg* operon encoding enzymes responsible for IPS synthesis and degradation (Harris et al., 1992) or pyruvate oxidation (*adhA-D*, *pfl2*) connected with acetate kinase

(*ackA*) involved in acetate production from pyruvate, yielding an additional ATP compared with lactate production (Figure 5b). Interestingly, the presence of xylitol blocked acetate production by the cells more than the TSB medium without any carbohydrates, as well as further downregulated the ribosomal genes (Figure 4c). Between culturing the cells with lactose and xylitol, the only difference in carbohydrate metabolism was observed in the galactose catabolism by the tagatose pathway and the Leloir pathway (Figure 4). The genes of the Leloir pathway (SMU_886-88) inducible by extra- or intracellular galactose released from α -galactoside were upregulated on both lactose and xylitol. However, the genes for the tagatose pathway (SMU1490-96), which are induced only by lactose (Zeng et al., 2010), were exclusively upregulated on lactose (Figure 5b).

3.2.2 | Expression levels of genes for two-component systems, competence, and virulence

From 14 two-component systems (TCS) described in *S. mutans* UA159, we found transcripts for 13 of them (Figure 5c). A more pronounced difference in expression was observed in the case of TCS-10 (SMU_576-577), represented by the genes for HK-LytS and RR-LytT. The TCS-10 was significantly downregulated on glucose versus sucrose and upregulated on lactose versus xylitol (Figure 5c). Its expression induced

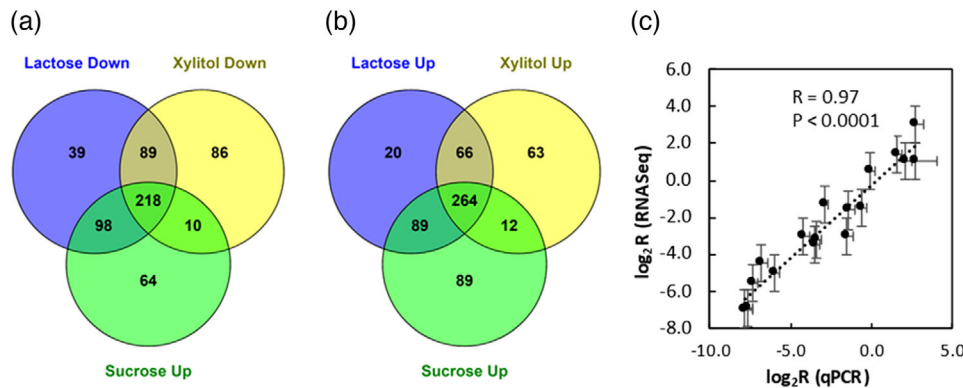


FIGURE 3 Overlap between genes expressed in *Streptococcus mutans* cells treated with lactose, xylitol, and sucrose. (a) The Venn diagram of the overlap between downregulated genes on lactose and xylitol and upregulated genes on sucrose shows 226 common significantly changed genes. (b) The Venn diagram of the overlap between upregulated genes on lactose and xylitol and downregulated genes on sucrose shows 270 common significantly changed genes. A >1.5 -fold difference and $p_{\text{adj}} < 0.05$ were used as the cutoff. (c) Validation of RNA-Seq data by the RT-qPCR method on 10 candidate genes representing genes with a large change ($\log_2 \text{FoldChange} \approx 6$), medium change ($\log_2 \text{FoldChange} \approx 3$), small change ($\log_2 \text{FoldChange} \approx 1.5$), and no change ($\log_2 \text{FoldChange} \approx 0.1$) in expression related to tryptone soya broth (TSB) in the samples cultivated on glucose, sucrose, lactose, and xylitol (see Table S1).

the expression of many PTS and genes involved in carbohydrate metabolism and repressed bacteriocins (Figure 5d). The same trends were also observed for TCS-7 (SMU_1037-1038c; HKPhoR and RR-YcbL) between sucrose and lactose versus xylitol (Figure 5c), whose exact role has not been described yet. The opposite trends were observed in the regulation of TCS-4 (SMU_927-928; HK-KinF and RR-LlrF) involved in acid tolerance and (p)ppGpp metabolism in *S. mutans* (Zhang et al., 2020). The specific upregulation of the four-component regulatory system TCS-9 (SMU_1963-1966c), including HK-LevS, RR-LevR, and carbohydrate-binding proteins LevQT, in the cells growing with sucrose was consistent with its function in regulating fructan hydrolase genes (*fruA*) (Zeng et al., 2011) (Figure 5c).

Between the cells growing with glucose versus sucrose and lactose versus xylitol, we observed the opposite expression of *comC* (SMU_1915), the precursor for competence-stimulating peptide (CSP), together with the late competence genes *comEA* (SMU_625) and *comEC* (SMU_626) (Figure 5e). Furthermore, the observed upregulation of *comC* on glucose versus sucrose corresponded to the expression of small antimicrobial peptides termed mutacins (Figure 5d) regulated mainly by the CSP-ComDE system and TCS-2 (SMU_1128-1129) represented by HK-CiaH and RR-CiaR involved in competence development, sucrose-dependent biofilm formation, and acid tolerance (Qi et al., 2004). Noticeably, the other late competence genes *comYB* (SMU_1985) and *comYD* (SMU_1983) showed upregulation only in the cells growing with glucose and correlated with the expression of the LevQRST signal transduction complex (TCS-9) (Figure 5e). Surprisingly, the genes encoding the GTFs GtfB (SMU_1004) and GtfC (SMU_1005) and sucrose phosphorylase GtfA (SMU_881), which play a crucial role in the synthesis of EPS by providing the matrix for biofilm formation (Ren et al., 2016), were downregulated in the cells growing with glucose and sucrose but upregulated in the cells growing with lactose and xylitol (Figure 5f). By contrast, other gene expressions related to EPS synthesis, such as *gtfD* (SMU_910), *sacB* (SMU_2028),

and *vicR* (SMU_1517), were almost unchanged under all conditions (Figure 5c,f).

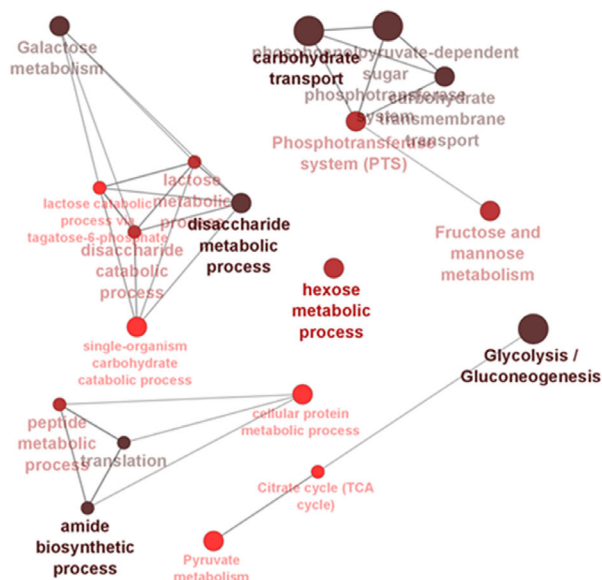
3.2.3 | Expression levels of genes involved in cell wall synthesis

The cell wall of *S. mutans* is highly decorated by rhamnose-glucose polysaccharides (RGPs). The cell growth with lactose or xylitol resulted in significant downregulation of the *rgp* operon (SMU_824-33; Figure 5f). However, the presence of glucose or sucrose in the medium significantly upregulated several genes of the *rgp* operon (Figure 5e). Namely, the gene *rgpI* (SMU_833) encoding GTF was upregulated on both carbohydrates, while the genes *rmID* (SMU_824), *rgpA* (SMU_825), and *rgpD* (SMU_828) were upregulated only on sucrose, and the gene *rgpF* (SMU_830) encoding rhamnosyltransferase was upregulated only on glucose (Figure 5f). The regulation of the *rpg* operon positively correlated with the expression of TCS-4 (HK-KinF and R-LlrF), *comC*, *comEA*, *comEC*, and mutacins but negatively correlated with the expression of TCS-7 (HK-PhoR and RR-YcbL), TCS-10 (HK-LytS and RR-LytT), and *gtfA-gtfC* or *gbpC* genes related to EPS synthesis involved in biofilm formation and cell wall metabolism (Figure 5c,f).

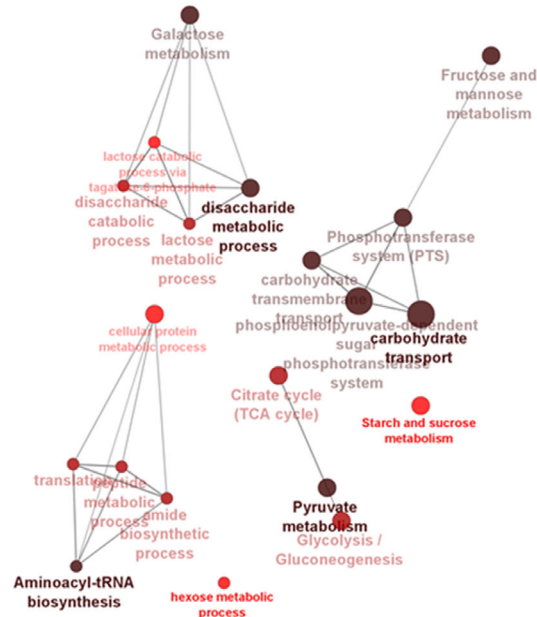
3.3 | Changes in metabolites involved in *S. mutans* cell wall synthesis

Transcriptomic analysis was combined with the analysis of metabolites related to cell wall synthesis. The PCA from 611 metabolites that differed between the samples with a fold change > 10 and $p < 0.001$ provided a visual representation of the metabolite similarities between the cells growing in a medium without carbohydrates and with individual carbohydrates. Except for the cells growing with xylitol,

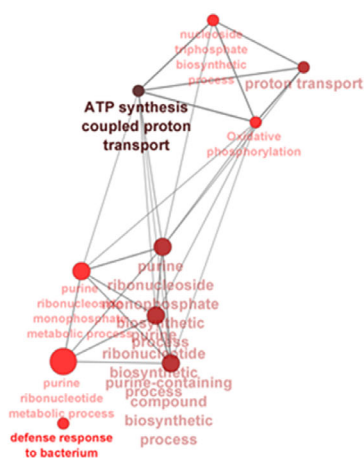
(a) Sucrose Down-regulated



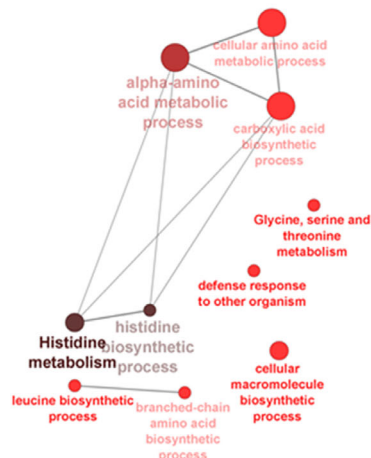
(b) Lactose Up-regulated



(e) Sucrose Up-regulated



(d) Glucose Up-regulated



(c) Xylitol Down-regulated

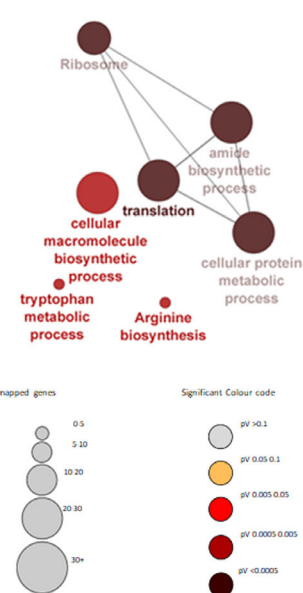


FIGURE 4 Biological processes and KEGG pathways likely to be regulated by different carbohydrates and xylitol. Gene ontology (GO) analysis was performed using the ClueGo Cytoscape plug-in. A list of unique genes was generated from the statistically significant regulated transcripts (>1.5 -fold change and $p_{adj} < 0.05$). Each list was used to query the KEGG and Gene Ontology biological process database. The ClueGo parameters were set as indicated: Go Term Fusion selected; only display pathways with p -values ≤ 0.05 ; GO tree interval, all levels; GO term minimum # genes, 2; threshold of 4% of genes per pathway; and kappa score of 0.40. The GO terms are presented as nodes and clustered together based on the similarity of the genes present in each term or pathway.

individual replicates growing with the different carbohydrates clustered separately, indicating distinctive metabolic profiles (Figure 6a). Noticeably, the cells growing with glucose differed significantly from those growing with sucrose, lactose, or xylitol. Ten differential metabolites related to cell wall synthesis were identified (Figure 7). In the cells growing without carbohydrates or with xylitol, the concentrations of

dTDP-L-rhamnose needed to produce structurally similar rhamnose polysaccharides in the cell wall (van der Beek et al., 2019) were significantly reduced. Similarly, the key intermediates of bacterial peptidoglycan biosynthesis represented by UDP-MurNAc, UDP-MurNAc-L-Ala, UDP-MurNAc-L-Ala-D-Glu, UDP-MurNAc-pentapeptide, and dTDP-L-rhamnose were significantly reduced in these cells (Figure 7).

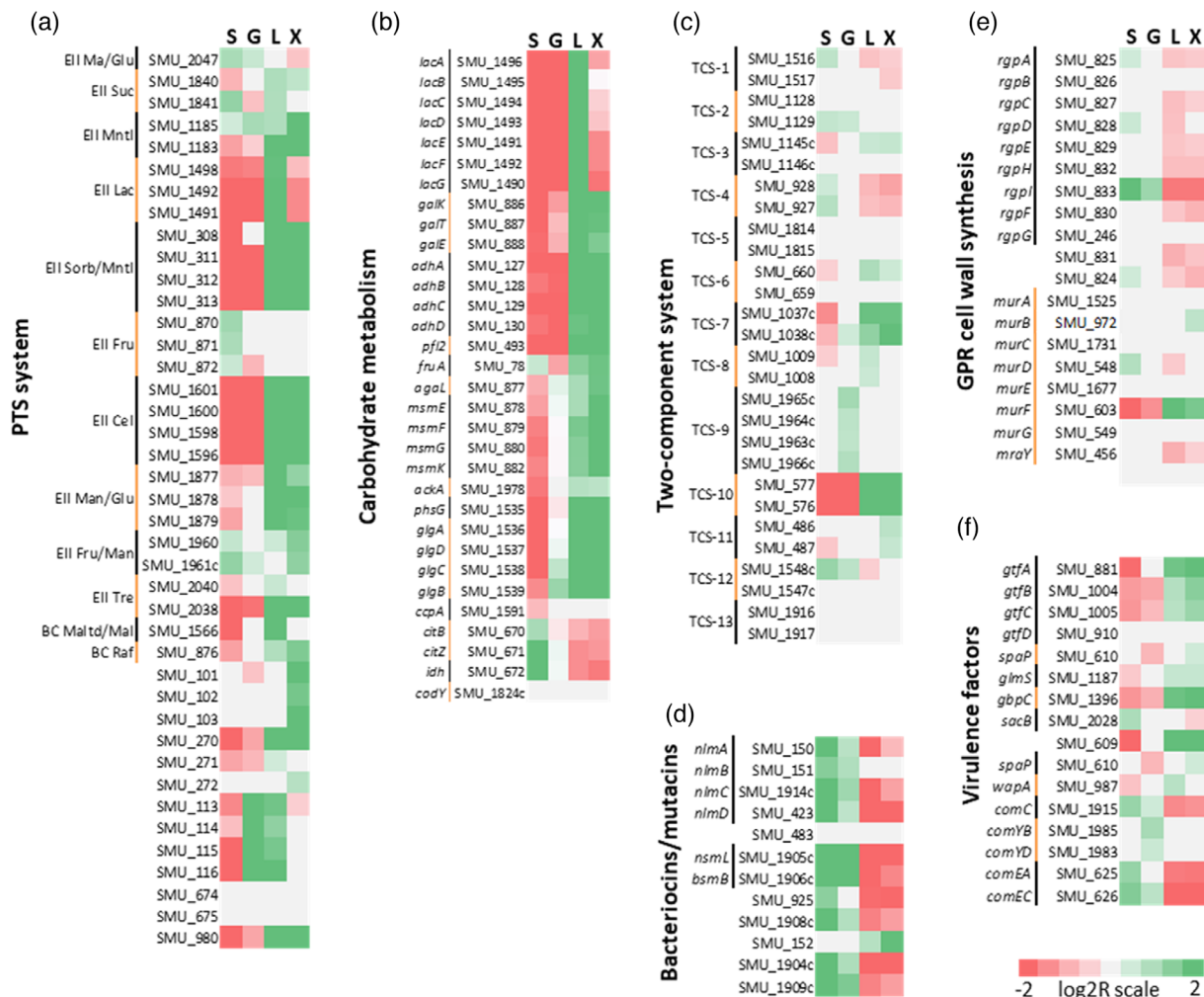


FIGURE 5 Differentially expressed genes related to carbohydrate metabolism and the virulence of *Streptococcus mutans*. Heat maps of genes related to phosphotransferase system (PTS) (a), carbohydrate metabolism (b), two-component signaling (c), bacteriocins production (d), cell wall synthesis (e), and virulence (f). The colors show different expression data according to the \log_2 FoldChange (\log_2R) value with $p_{adj} < 0.05$. The shades of red represent downregulations of transcripts, gray stands for no change, and the shades of green represent upregulations of transcripts.

Finally, we analyzed typical clumps observed during the planktonic cultivation of *S. mutans* with sucrose. We were unable to identify peptides by LC-MS/MS analysis after the lysis of bacterial cells from the clumps and excessive washing, and trypsin or Glu-C digestion (data not shown). HPLC analysis of the clumps for carbohydrate content after their acid hydrolysis and derivatization by PMP according to the method described by Rühmann et al. (2014) identified rhamnose, glucose, and ribose in a molar ratio of 0.17:0.27:0.56 (Figure 6b).

3.4 | The effect of different carbohydrates on *S. mutans* biofilm formation

The biofilm biomass formed by *S. mutans* on polystyrene well plates, tested by the crystal violet method, differed significantly between individual carbohydrates. In the presence of glucose and lactose, biofilm increased 2-fold, and even more in the presence of sucrose as compared with the control unsupplemented TSB medium (Figure 8a).

In agreement with the assumption, the addition of xylitol did not significantly affect biofilm formation by *S. mutans* (Figure 8a).

To further characterize the effect of used carbohydrates on biofilm formation by *S. mutans*, the structure of the biofilm was analyzed using CLSM (Figure 8b) and SYPRO® Ruby biofilm matrix stain. The matrix density in TSB and TSB supplemented with xylitol showed less density and contained fewer bacteria in comparison with the addition of glucose, lactose, or sucrose (Figure 8b). Specifically, the matrix grown in the presence of sucrose was further characterized by densely clustered microcolonies (Figure 8b).

4 | DISCUSSION

Although many previous studies have evaluated the effects of carbohydrates on the *S. mutans* transcriptome, not all benefited from detailed RNA-Seq analysis, and most studies compared the effects of individual carbohydrates on the *S. mutans* transcriptome in the presence of

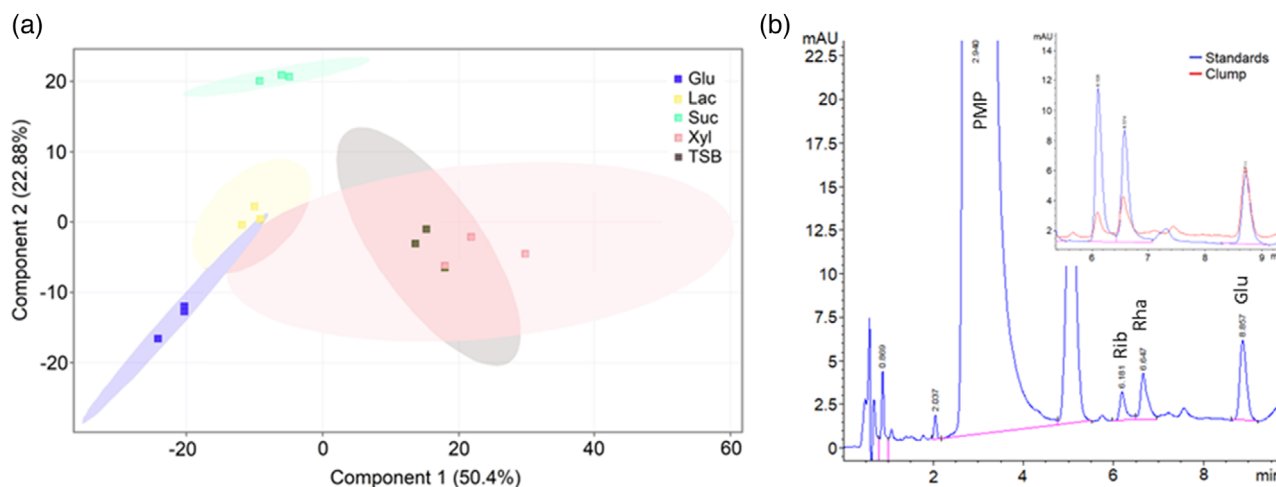


FIGURE 6 Overall metabolomic changes associated with the cultivation of *Streptococcus mutans* on different carbohydrates and xylitol. (a) Principal component analysis (PCA) plot from 611 metabolites that differed between the samples with $p < 0.05$, showing clustering of the samples: gray—no carbohydrates (tryptone soya broth [TSB]), purple—xylitol, yellow—lactose, green—sucrose, and red—glucose. (b) HPLC chromatogram of the carbohydrate composition of clumps originated during the growth of *S. mutans* on sucrose. The inset represents the details of the overlay chromatograms of the sample (red) and combined standard (blue); 50 $\mu\text{g}/\text{mL}$ rhamnose, 50 $\mu\text{g}/\text{mL}$ glucose, and 50 $\mu\text{g}/\text{mL}$ ribose. The Agilent 1200 Infinity Series (Agilent Technologies) was used for the analysis of the samples after derivatization with 1-phenyl-3-methyl-5-pyrazolone (PMP), with a diode array detector (detected wavelengths of 210 and 245 nm).

endogenous glucose in the culture medium (Decker et al., 2014; He et al., 2017; Zeng & Burne, 2016; Zeng et al., 2010) because this microorganism lacks a complete respiratory chain and cannot grow in the absence of carbohydrates. In this study, a planktonic culture model and RNA-Seq described the transcriptional changes preceding the transition from a planktonic existence to biofilm development. The nutritional status of the environment partly regulates this transition. Therefore, we implemented the growth of *S. mutans* under fasting conditions (medium without carbohydrates), relatively high concentrations of preferred carbohydrates (0.5% glucose or 0.5% sucrose) and nonpreferred carbohydrates (0.5% lactose), and nonfermentable polyol xylitol with a predicted growth inhibitory effect.

4.1 | IPS metabolism

Under fasting conditions, there was no observable growth of the *S. mutans* culture, but we detected acetic acid production as a byproduct of its metabolic processes without a significant drop in pH in the culture media (Figure 1). This situation corresponded to limiting the carbohydrate conditions of mixed-acid fermentation when pyruvate is converted to acetyl-CoA instead of lactate and is further converted to acetate (Willenborg & Goethe, 2016) to regenerate NADH for biosynthetic reactions. IPSs, glycogen-like molecules composed primarily of α -1,4-linked glucose polymers (Busuic et al., 2009; Wilson et al., 2010), are proposed to form in cells during carbohydrate starvation and may play an essential role in *S. mutans* survival. Glycogen phosphorylase activity can hydrolyze IPS and release glucose as G6P (Busuic et al., 2009; Costa Oliveira et al., 2021; Wilson et al., 2010), as we observed by the upregulation of glycogen phosphorylase PhsG

(SMU_1535) in the cells growing with lactose or xylitol. Thus, IPS extends the duration of acid production, as reported here, and contributes to the cariogenicity of *S. mutans* in animal models (Spatofora et al., 1995). The observed current regulation of the *glg* operon (SMU_1535-39) supported previously described co-expressions of mRNAs for both biosynthetic and degradative enzymes and confirmed the previous suggestion that actual physiological parameters reflected in the levels of metabolic intermediates, such as G6P, G1P, ADP, and Pi, may have a direct function in regulating IPS metabolism (Costa Oliveira et al., 2021). Another possibility may be that the pullulanase PulA (SMU_1541) has a significant role in modifying the IPS structure and persistence under starvation conditions (Busuic et al., 2009) and whose expression was elevated only in the cells growing with lactose or xylitol. Interestingly, the *glg* operon was exclusively downregulated in the cells growing with sucrose and not with glucose. It confirmed the previous finding that sucrose metabolism employing extracellular sucrolytic enzymes alters the expression of the *glg* operon in a manner that modulates IPS accumulation (Costa Oliveira et al., 2021).

4.2 | The reprogramming of metabolism according to carbohydrate source

TCS are an important mode of signal transduction in *S. mutans* during adaptation to external stimuli (Mattos-Graner & Duncan, 2017). Therefore, TCS play a vital function in coordinating bacterial growth with virulence function for persistence at the host site (Mattos-Graner & Duncan, 2017). In our case, a different reprogramming between high-energy carbohydrates (sucrose or glucose) and a low-energy carbohydrate (lactose) together with nonfermentable polyol (xylitol) is

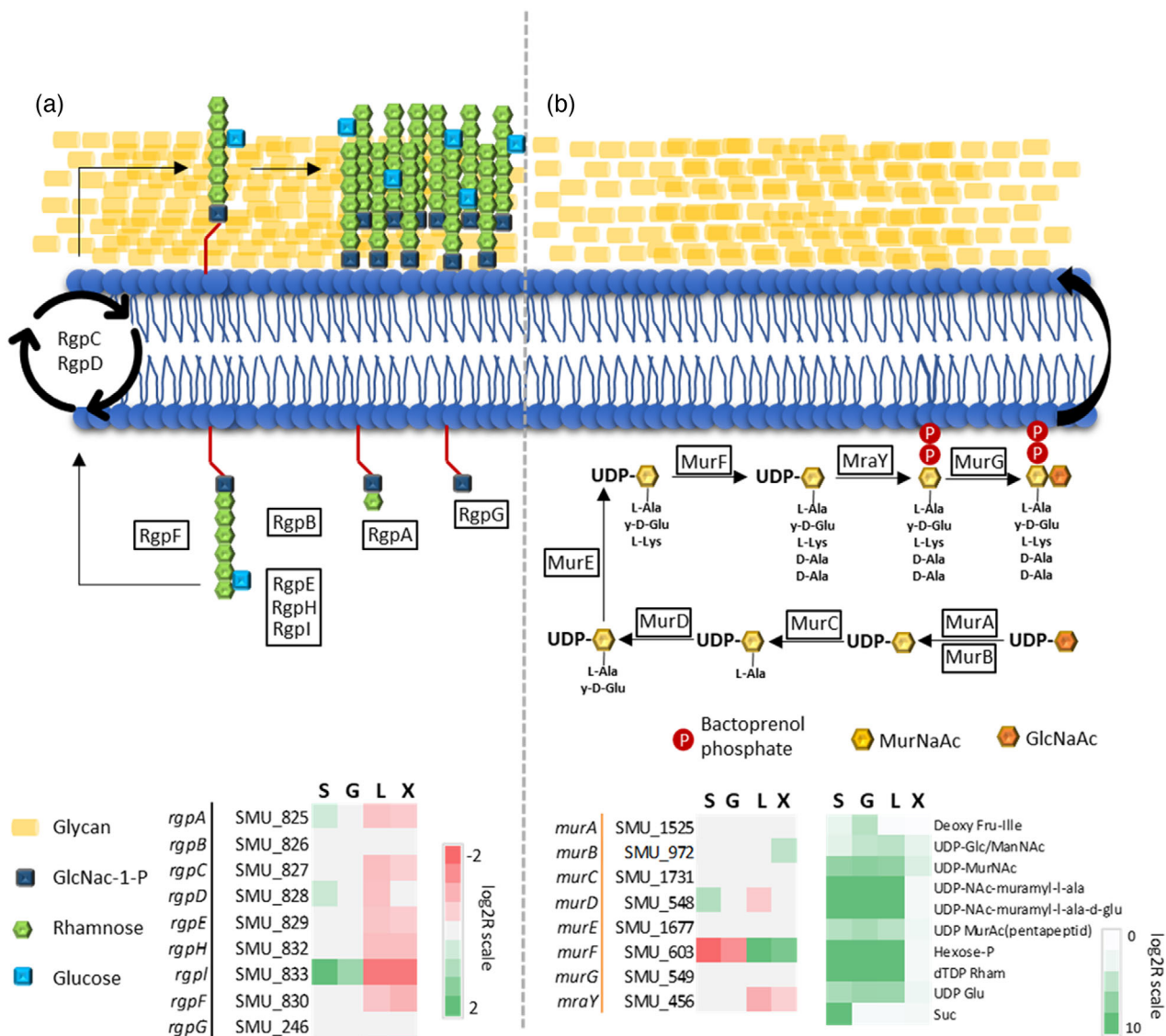


FIGURE 7 Rhamnose–glucose polysaccharide (RGP) and peptidoglycan formation in *Streptococcus mutans*. The formation steps corresponding to RGP (a) and peptidoglycan (b) biosynthesis are displayed together with differentially expressed genes and levels of metabolites significantly changed in metabolomic analysis related to peptidoglycan synthesis. The colors show the expression/concentration levels relative to those in no-carbohydrate control and are expressed as log₂R ratios of the relative change. The shades of red represent the downregulation of transcripts, gray stands for no change, and the shades of green represent the upregulation of transcripts/metabolites.

connected with the *S. mutans* transduction system TCS-10 comprising a transmembrane histidine kinase LytS (SMU_577) and cytoplasmic response regulator LytT (SMU_576) (Song et al., 2012) involved in biofilm formation and cell wall metabolism (Ahn et al., 2010; Chong et al., 2008). The *lytST* operon is conserved in a subset of gram-positive bacterial genera, including *Staphylococcus* (Bayles, 2007). The LytST two-component regulatory system has been shown to positively regulate the *S. mutans* expression of LrgA/B holin-like proteins sharing structural features with the bacteriophage-encoded holin family and playing a role in autolysis, biofilm formation, and oxidative stress tolerance (Ahn et al., 2010, 2012). Analysis of the operator sequence in low-GC gram-positive bacteria has shown that LytST affects or regulates the transport of carbohydrates, peptides, and amino acids (de

Been et al., 2008). It supported our observed data and showed the hierarchical regulation of the Lrg system in a signaling network involving carbohydrate availability. The regulation of the Lrg system is much more pronounced during low-oxygen growth and at low glucose levels (Ahn et al., 2012), which supported the high upregulation of the *lrgAB* operon (SMU_575c/574c) (more than 60-fold) in the cells growing with xylitol and lactose (Figure 5). Interestingly, the consensus cAMP response element (CRE), which is a binding site for CcpA (carbon catabolite protein A), is located directly upstream of the *lytST* operon (Figure 9), and two putative CRE sequences have been previously identified in the *lrg* promoter in *S. mutans* (Ahn et al., 2010). It could explain a strong downregulation of the *lytST* operon in the cells growing with glucose or sucrose. In addition, the *lrgAB* operon was strongly

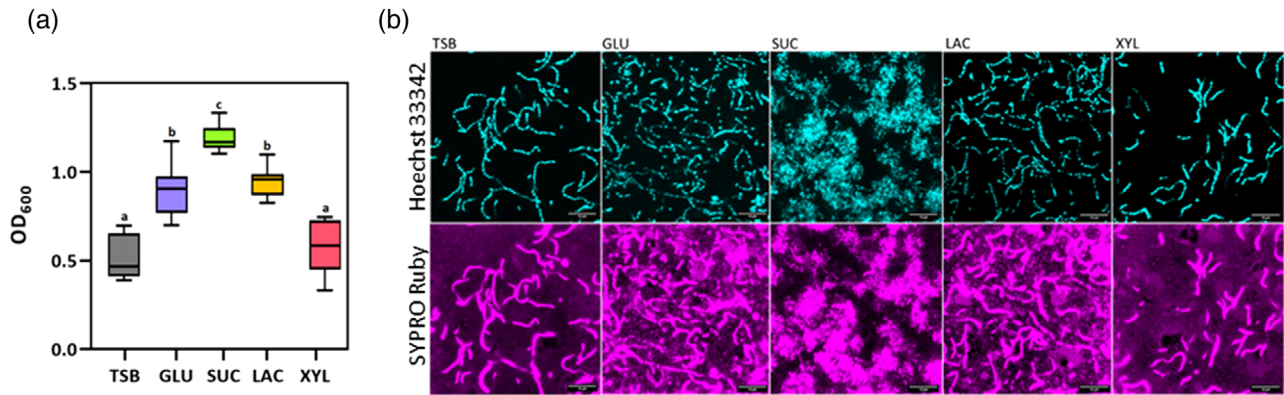


FIGURE 8 Quantification and characterization of biofilm biomass and matrix. (a) The biofilms formed using tryptone soya broth (TSB) and TSB supplemented with 0.5% glucose (GLU), sucrose (SUC), lactose (LAC), and xylitol (XYL) were quantified using crystal violet staining. The data represent two independent biological experiments, each performed in tetraplicates. Error bars indicate the 95% confidence interval; statistical significance was analyzed by analysis of variance and Dunnett's post hoc test and is denoted by letters ($p < 0.01$). (b) Staining with Hoechst 33342 (cell-permeant nucleic acid stain) and SYPRO Ruby (a dye that stains both cell wall and matrix) reveals a higher bacteria count and denser matrix in biofilm formed in TSB medium supplemented with 0.5% glucose (GLU), sucrose (SUC), and lactose (LAC). All images were obtained at the same confocal laser scanning microscopy settings.

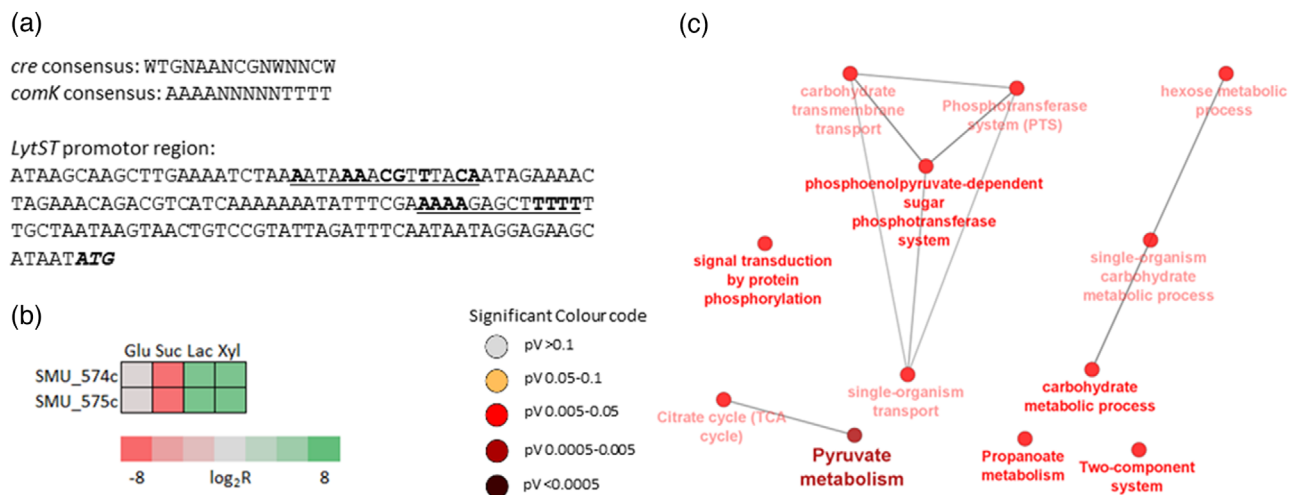


FIGURE 9 *LysT* two-component regulatory system. (a) Identification of *cre* and *comK* sequences upstream of *lysT*. The nucleotide sequence corresponding to 143 bp upstream of the ATG start codon (identified in bold italics) of the *Streptococcus mutans lysT* gene is shown at the bottom. The putative *cre* and *comK* elements are underlined, and the conserved nucleotides are shown in bold. (b) Expression of *IrgAB* (SMU_575c/574c) on different carbohydrates related to tryptone soya broth (TSB) without carbohydrates, log₂FoldChange (log₂R) value with $p_{adj} < 0.05$. The shades of red represent the downregulation of transcripts, gray stands for no change, and the shades of green represent the upregulation of transcripts. (c) Common biological processes and KEGG pathways downregulated in mutant strains *lysT*⁻ and *IrgAB*⁻ of *S. mutans* (Ahn et al., 2012; Rice et al., 2017) and on sucrose treatment and upregulated after lactose and xylitol treatment. Each list was used to query the KEGG and Gene Ontology biological process database. The ClueGo parameters were set as indicated: Go Term Fusion selected; only display pathways with p values ≤ 0.05 ; GO tree interval, all levels; GO term minimum # genes, 2; threshold of 4% of genes per pathway; and kappa score of 0.40. The gene ontology terms are presented as nodes and clustered together based on the similarity of the genes present in each term or pathway.

downregulated (more than 60-fold) exclusively in the cells growing with sucrose, indicating its more complex regulation with a possible role for metabolites, as suggested previously (Ahn et al., 2012; Rice et al., 2017). A comparison of our transcriptomic data with previously reported data from the mutant strains *lysT*⁻ and *IrgAB*⁻ (Ahn et al., 2012; Rice et al., 2017) showed the intersection in the processes and pathways related to energy metabolism and carbohydrate transport

regulated through individual genes (*lysT*, *IrgAB*) and highlighted the role of TCS-10 in carbohydrate transport and metabolism (Figure 9C).

Concerning carbohydrate metabolism, sucrose has a distinct behavior due to the notable clumping of the *S. mutans* cells, a phenotype resembling biofilm. This phenotype is associated to a large extent with the activity of secreted sucrolytic enzymes converting sucrose to free glucose and fructose that impact the cells at the transcriptomic level

(Zeng & Burne, 2016). Besides, the phenomenon of fructose expulsion after the internalization of sucrose can also contribute to this behavior of sucrose. The most apparent observation in sucrose compared to lactose and xylitol was the massive downregulation of glycolytic enzyme transcripts and carbohydrate metabolic processes (Figure 4a) that were already proved on the protein level during the acid tolerance response of *S. mutans* (Welin et al., 2003). This altered metabolic flow can be seen as a protective measure to limit further acidification by the formation of lactic acid in planktonic culture supplemented with sucrose and to increase the pool of glycolytic intermediates for biosynthetic processes represented by regulation of genes involved in amino acid synthetic pathways and translation. In addition, the observed downregulation of genes *pfl*, *ackA*, *pycB*, *cil*, or *citC* on sucrose indicates a reduction in a pyruvate metabolism pathway that results in acetate and ATP production. This pathway specifically dominates under carbohydrate-limiting conditions, which is supported by its upregulation in the presence of lactose and xylitol.

4.3 | The opposing effects of carbohydrates on genes for virulence and competence

Based on the results of this study, there is clear evidence that carbohydrate sources have a strong influence on genes network associated with acid tolerance and genetic competence. The slightly upregulated *ciaRH* operon (SMU_1128-29) encoding TCS-2 in the cells growing with glucose or sucrose has been previously implicated in acid tolerance, sucrose-dependent biofilm formation, and mutacin production (Qi et al., 2004). Furthermore, the upregulation of *ciaR* has also been found in early-stage interaction with *Candida albicans* (He et al., 2017). The more dramatic differences in gene expression between typical cariogenic carbohydrates (sucrose, glucose) and lactose versus xylitol-grown cells were noted. The feedback regulation of the *comC* gene, which encodes CSP, as well as late competence genes (*comEA* and *comEC*) and small antimicrobial peptides referred to as mutacins. The development of genetic competence is pH sensitive and influenced by biofilm formation, stress tolerance, or extracellular DNA release (Son et al., 2015). The upregulation of these competence genes was consistent with earlier findings that the presence of sucrose in a medium increases the chance of *S. mutans* acquiring foreign DNA as a nutrient source or enhancing genome diversification (Zeng & Burne, 2016). Indeed, the CSP-ComDE system regulates mutacin expression (van der Ploeg, 2005), as observed here. The expression of mutacins is considered necessary in competing with early colonizers during biofilm formation (Merritt & Qi, 2012). So, their reduced expression in the cells growing with lactose or xylitol may have altered the microbial composition of the oral biofilm and promoted a symbiotic relationship between *S. mutans* and *C. albicans* during biofilm formation (He et al., 2017). In addition, lactose at relevant concentrations in dairy products even enhances the adhesion of *S. mutans* during the initial steps of biofilm formation (Assaf et al., 2015).

Here, acetic acid production and biofilm formation was largely abolished in the presence of xylitol in the growth medium, confirming the

previously described inhibitory effect of xylitol under experimental conditions in the absence of other fermentable carbohydrates (Decker et al., 2014). This effect is believed to be related to the energy-consuming futile cycle of xylitol uptake by fructose PTS encoded by *fruI* (SMU_114) (Tanzer et al., 2006) and disruption of protein synthesis (Trahan et al., 1991), which we demonstrated by the downregulation of the genes involved in the translation process (Figure 4). The enhanced futile cycle of xylitol uptake was further augmented by a significant xylitol-induced reprogramming of the *S. mutans* transcriptome nearly identical to the presence of lactose and inverse to the presence of sucrose in the growth medium. This reprogramming involved the upregulation of most genes for PTS and carbohydrate metabolism, except lactose metabolism, and the downregulation of the genes catalyzing the synthesis of 2-oxoglutarate from acetyl-CoA by the fragmentary tricarboxylic acid (TCA) cycle, the role of which in streptococci is still limited (Willenborg & Goethe, 2016). Noticeably, the expression of these genes has been previously reported to be downregulated in response to acid stress. This adaptation was proposed to minimize the synthesis of amino acid precursors and promote citrate metabolism to pyruvate, allowing H⁺ consumption and ATP synthesis (Chen et al., 2010). Moreover, 2-oxoglutarate represents an essential precursor of amino acids of the glutamate family, and the fragmentary TCA cycle allows the generation of additional NADPH. However, the presence of xylitol and lactose in the growth medium upregulated many virulence factors, which supported the previous observation that simultaneous exposure to xylitol and glucose has a no-inhibitory effect on *S. mutans* biofilm activity in terms of vitality, respiratory activity, or EPS production needed for bacterial adhesion under stress conditions (Decker et al., 2014). Besides, the observed upregulation of many biofilm-related genes in lactose and xylitol exhibiting different trends in the reduction of pH showed that both carbohydrates act as global signal molecules for their regulation, as suggested before for lactose (Decker et al., 2014). On the other hand, despite the similarities in transcriptome changes between lactose and xylitol, there was no overlap in metabolomes and the biofilm formation was observed only in the case of lactose. In the case of the metabolome, this could be explained by the energy-consuming futile cycle of xylitol uptake resulting in massive transcriptome reprogramming without consequent metabolic activity due to a lack of substrates and energy sources. The difference in biofilm formation could be explained by different changes in pH values or bacterial growth when the results of previous studies stress a more important role of pH change compared to bacterial growth (Loo et al., 2000). It was previously demonstrated that the EPS profile of biofilm formed in the presence of lactose is different from that formed in sucrose (Assaf et al., 2015). However, the growth of biofilm and EPS production were similar to sucrose or glucose (Decker et al., 2014). This result is consistent with our observed downregulation of the genes involved in synthesizing RGP cell wall structures in the presence of lactose or xylitol and biofilm growth and morphology analyzed by CLSM. The most significant change in expression showed the *rgpI* gene controlling the branching frequency of the side-chain linkage (Ozaki et al., 2002). RGPs are essential in many cellular processes, including cell division or tolerance to harsh

environmental conditions (Kovacs et al., 2019). The *rgp* mutant strains showed striking defects in cellular morphology and slightly impaired growth, especially under stress conditions (Kovacs et al., 2019). Interestingly, the *S. mutans* serotype *k* carrying the insertional mutation in the *rgpE* gene is the least frequent in cariogenic lesions among the different infectious *S. mutans* serotypes (Nomura et al., 2005). The *murF* gene exhibited opposite regulation to the *rgpI* gene. This gene is involved in peptidoglycan biosynthesis for bacterial cell walls, and the bacteria with altered transcription exhibited slower growth and reduced beta-lactam antibiotic resistance (Sobral et al., 2006). A previous study modulating *murF* expression in *S. aureus* cells showed that a reduced transcription rate causes alterations in many genes (Sobral et al., 2007). Indeed, the modulation of *murF* expression had a selective effect on the transcription of virulence-related genes, most of which were overexpressed when *murF* transcription was suboptimal (Sobral et al., 2007). All these observations may lead to speculations on how the downregulation of RGPs and upregulation of *murF* may affect pathogenicity in the presence of lactose or xylitol.

5 | CONCLUSION

The present study provided a comprehensive insight into *S. mutans* transcriptomic changes associated with growth in the presence of carbohydrates with different cariogenic effects, which depend mainly on how efficiently a respective carbohydrate can be metabolized by the glycolytic pathway and thus induce acidification and promote demineralization of hard dental tissues. Previous research on *S. mutans* revealed profound impacts of individual carbohydrates on the physiology and gene expression of this bacterium that was associated with dental caries in both primary and permanent dentition. Here, the planktonic culture model and RNA-Seq described the transcription changes preceding the transition from a planktonic existence to biofilm development under fasting conditions and the conditions of preferred and nonpreferred carbohydrates. Interestingly, *S. mutans* in the planktonic culture with lactose produced the same pH drop as glucose and sucrose. However, the presence of lactose or xylitol in the growth medium resulted in a contrasting transcription pattern compared with sucrose and glucose, which affected IPS metabolism, competition with early colonizers for dental biofilm formation and structure, and tolerance to harsh environmental conditions. Previous studies also found that milk sugar lactose and polyol xylitol have a protective effect on biofilm formation. Nevertheless, the high efficacy of xylitol in the regulating genes associated with IPS and biofilm, similar to lactose, tended to confirm the results of recent studies that xylitol (in the presence of glucose or sucrose) and lactose may play a vital role in biofilm composition and structure but do not reduce its formation. Furthermore, the role of preferred and nonpreferred carbohydrates for oral microorganisms in the initial phase of biofilm formation and their role in modulating its cariogenic environment should be further investigated using advanced omics techniques.

AUTHOR CONTRIBUTIONS

Jan Lochman, Jiri Kucera, and Petra Borilova Linhartova conceived the experiment. Jiri Kucera, Veronika Jurakova, and Katerina Paskova performed cultivation experiments and analyzed the results. Veronika Jurakova and Martina Zapletalova performed RNA-Seq experiments and analyzed the results. Veronika Farková, Veronika Jurakova, Katerina Dadakova, and Roman Reminek performed the analysis of metabolites and analyzed the results. Jan Lochman, Jiri Kucera, Katerina Dadakova, Petra Borilova Linhartova, and Veronika Jurakova drafted and co-wrote the paper. Filip Ruzicka, Lydie Izakovicova Holla, and Zdenek Glatz critically revised the manuscript. Petra Borilova Linhartova and Lydie Izakovicova Holla secured funding for the study. All authors revised the final version of the manuscript. Jan Lochman, Veronika Jurakova, Veronika Farková, Jiri Kucera, Katerina Dadakova, Martina Zapletalova, and Petra Borilova Linhartova gave final approval for the version to be published. Jan Lochman, Veronika Jurakova, Veronika Farková, Jiri Kucera, Katerina Dadakova, Martina Zapletalova, and Petra Borilova Linhartova agreed to be accountable for all aspects of the work in ensuring that questions related to the accuracy or integrity of any part of the work are appropriately investigated and resolved.

ACKNOWLEDGMENTS

This research was supported by the Ministry of Health of the Czech Republic (grant numbers: NV17-30439A and NU20-08-00205). V.J. and V.F. were supported by the Institutional Research Fund of Masaryk University (MUNI/A/1492/2021). This publication has received funding from the European Union's Horizon 2020 Research and Innovation Programme under grant agreement number 857560. This publication reflects only the authors' view, and the European Commission is not responsible for any use that may be made of the information it contains. The authors also thank the Research Infrastructure RECETOX RI (No. LM2018121) and project CETOCOEN EXCELLENCE (No. CZ.02.1.01/0.0/0.0/17_043/0009632) financed by the Ministry of Education, Youth, and Sports for supportive background. We acknowledge the core facility CELLIM supported by the Czech-Biolmaging large RI project (LM2023050 funded by MEYS CR) for their support in obtaining scientific data presented in this paper.

CONFLICT OF INTEREST STATEMENT

The authors declare no conflicts of interest.

DATA AVAILABILITY STATEMENT

The data that support the findings of this study are openly available in Gene Expression Omnibus at <https://www.ncbi.nlm.nih.gov/geo/> (reference number GSE207392).

ORCID

Veronika Jurakova  <https://orcid.org/0000-0002-5921-7015>

Jan Lochman  <https://orcid.org/0000-0003-4420-8842>

REFERENCES

- Ahn, S.-J., Qu, M.-D., Roberts, E., Burne, R. A., & Rice, K. C. (2012). Identification of the *Streptococcus mutans* LytST two-component regulon reveals its contribution to oxidative stress tolerance. *BMC Microbiology*, 12, 187. <https://doi.org/10.1186/1471-2180-12-187>
- Ahn, S.-J., Rice, K. C., Oleas, J., Bayles, K. W., & Burne, R. A. (2010). The *Streptococcus mutans* Cid and Lrg systems modulate virulence traits in response to multiple environmental signals. *Microbiology*, 156(Pt 10), 3136–3147. <https://doi.org/10.1099/mic.0.039586-0>
- Ajdic, D., McShan, W. M., McLaughlin, R. E., Savic, G., Chang, J., Carson, M. B., Primeaux, C., Tian, R., Kenton, S., Jia, H., Lin, S., Qian, Y., Li, S., Zhu, H., Najar, F., Lai, H., White, J., Roe, B. A., & Ferretti, J. J. (2002). Genome sequence of *Streptococcus mutans* UA159, a cariogenic dental pathogen. *Proceedings of the National Academy of Sciences of the United States of America*, 99(22), 14434–14439. <https://doi.org/10.1073/pnas.172501299>
- Assaf, D., Steinberg, D., & Shemesh, M. (2015). Lactose triggers biofilm formation by *Streptococcus mutans*. *International Dairy Journal*, 42, 51–57. <https://doi.org/10.1016/j.idairyj.2014.10.008>
- Balakrishnan, M., Simmonds, R. S., & Tagg, J. R. (2000). Dental caries is a preventable infectious disease. *Australian Dental Journal*, 45(4), 235–245. <https://doi.org/10.1111/j.1834-7819.2000.tb00257.x>
- Banas, J. A. (2004). Virulence properties of *Streptococcus mutans*. *Frontiers in Bioscience: A Journal and Virtual Library*, 9, 1267–1277. <https://doi.org/10.2741/1305>
- Bayles, K. W. (2007). The biological role of death and lysis in biofilm development. *Nature Reviews Microbiology*, 5(9), 721–726. <https://doi.org/10.1038/nrmicro1743>
- Busuioc, M., Mackiewicz, K., Buttaro, B. A., & Piggot, P. J. (2009). Role of intracellular polysaccharide in persistence of *Streptococcus mutans*. *Journal of Bacteriology*, 191(23), 7315–7322. <https://doi.org/10.1128/JB.00425-09>
- Chen, P.-M., Chen, Y.-Y. M., Yu, S.-L., Sher, S., Lai, C.-H., & Chia, J.-S. (2010). Role of GlnR in acid-mediated repression of genes encoding proteins involved in glutamine and glutamate metabolism in *Streptococcus mutans*. *Applied and Environmental Microbiology*, 76(8), 2478–2486. <https://doi.org/10.1128/AEM.02622-09>
- Choct, M., Dersjant-Li, Y., McLeish, J., & Peisker, M. (2010). Soy oligosaccharides and soluble non-starch polysaccharides: A review of digestion, nutritive and anti-nutritive effects in pigs and poultry. *Asian-Australasian Journal of Animal Sciences*, 23(10), 1386–1398. <https://doi.org/10.5713/ajas.2010.90222>
- Chong, P., Drake, L., & Biswas, I. (2008). LiaS regulates virulence factor expression in *Streptococcus mutans*. *Infection and Immunity*, 76(7), 3093–3099. <https://doi.org/10.1128/IAI.01627-07>
- Colby, S. M., & Russell, R. B. (1997). Sugar metabolism by mutans streptococci. *Journal of Applied Microbiology*, 83(S1), 80S–88S. <https://doi.org/10.1046/j.1365-2672.83.s1.9.x>
- Costa Oliveira, B. E., Ricomini Filho, A. P., Burne, R. A., & Zeng, L. (2021). The route of sucrose utilization by *Streptococcus mutans* affects intracellular polysaccharide metabolism. *Frontiers in Microbiology*, 12, 33. <https://doi.org/10.3389/fmicb.2021.636684>
- Darwin, WipaCharles, & Cord-Ruwisch, R. (2018). Concurrent lactic and volatile fatty acid analysis of microbial fermentation samples by gas chromatography with heat pre-treatment. *Journal of Chromatographic Science*, 56(1), 1–5. <https://doi.org/10.1093/chromsci/bmx086>
- de Been, M., Bart, M. J., Abee, T., Siezen, R. J., & Francke, C. (2008). The identification of response regulator-specific binding sites reveals new roles of two-component systems in *Bacillus cereus* and closely related low-GC Gram-positives. *Environmental Microbiology*, 10(10), 2796–2809. <https://doi.org/10.1111/j.1462-2920.2008.01700.x>
- Decker, E.-M., Klein, C., Schwindt, D., & von Ohle, C. (2014). Metabolic activity of *Streptococcus mutans* biofilms and gene expression during exposure to xylitol and sucrose. *International Journal of Oral Science*, 6(4), 195–204. <https://doi.org/10.1038/ijos.2014.38>
- Depke, T., Franke, R., & Brönstrup, M. (2017). Clustering of MS2 spectra using unsupervised methods to aid the identification of secondary metabolites from *Pseudomonas aeruginosa*. *Journal of Chromatography B: Analytical Technologies in the Biomedical and Life Sciences*, 1071, 19–28. <https://doi.org/10.1016/j.jchromb.2017.06.002>
- Depke, T., Thöming, J. G., Kordes, A., Häussler, S., & Brönstrup, M. (2020). Untargeted LC-MS metabolomics differentiates between virulent and avirulent clinical strains of *Pseudomonas aeruginosa*. *Biomolecules*, 10(7), 1041. <https://doi.org/10.3390/biom10071041>
- Duarte, S., Klein, M. I., Aires, C. P., Cury, J. A., Bowen, W. H., & Koo, H. (2008). Influences of starch and sucrose on *Streptococcus mutans* biofilms. *Oral Microbiology and Immunology*, 23(3), 206–212. <https://doi.org/10.1111/j.1399-302X.2007.00412.x>
- Falsetta, M. L., Klein, M. I., Colonne, P. M., Scott-Anne, K., Gregoire, S., Pai, C.-H., Gonzalez-Begne, M., Watson, G., Krysan, D. J., Bowen, W. H., & Koo, H. (2014). Symbiotic relationship between *Streptococcus mutans* and *Candida albicans* synergizes virulence of plaque biofilms *in vivo*. *Infection and Immunity*, 82(5), 1968–1981. <https://doi.org/10.1128/IAI.00087-14>
- Harris, G. S., Michalek, S. M., & Curtiss, R. (1992). Cloning of a locus involved in *Streptococcus mutans* intracellular polysaccharide accumulation and virulence testing of an intracellular polysaccharide-deficient mutant. *Infection and Immunity*, 60(8), 3175–3185. <https://doi.org/10.1128/iai.60.8.3175-3185.1992>
- He, J., Kim, D., Zhou, X., Ahn, S.-J., Burne, R. A., Richards, V. P., & Koo, H. (2017). RNA-Seq reveals enhanced sugar metabolism in *Streptococcus mutans* co-cultured with *Candida albicans* within mixed-species biofilms. *Frontiers in Microbiology*, 8, 1036. <https://doi.org/10.3389/fmicb.2017.01036>
- Huang, R., Li, M., & Gregory, R. L. (2011). Bacterial interactions in dental biofilm. *Virulence*, 2(5), 435–444. <https://doi.org/10.4161/viru.2.5.16140>
- Islam, B., Khan, S. N., & Khan, A. U. (2007). Dental caries: From infection to prevention. *Medical Science Monitor: International Medical Journal of Experimental and Clinical Research*, 13(11), RA196–203.
- Koo, H., Xiao, J., Klein, M. I., & Jeon, J. G. (2010). Exopolysaccharides produced by *Streptococcus mutans* glucosyltransferases modulate the establishment of microcolonies within multispecies biofilms. *Journal of Bacteriology*, 192(12), 3024–3032. <https://doi.org/10.1128/JB.01649-09>
- Kovacs, C. J., Faustoferri, R. C., Bischer, A. P., & Quivey, R. G. (2019). *Streptococcus mutans* requires mature rhamnose-glucose polysaccharides for proper pathophysiology, morphogenesis and cellular division. *Molecular Microbiology*, 112(3), 944–959. <https://doi.org/10.1111/mmi.14330>
- Krzysciak, W., Jurczak, A., & Piątkowski, J. (2016). The role of human oral microbiome in dental biofilm formation. In D. Dhanasekaran & N. Thajudhin (Eds.), *Microbial biofilms—Importance and applications* (pp. 329–382). IntechOpen. <https://doi.org/10.5772/63492>
- Kucera, J., Lochman, J., Bouchal, P., Pakostova, E., Mikulasek, K., Hedrich, S., Janiczek, O., Mandl, M., & Johnson, D. B. (2020). A model of aerobic and anaerobic metabolism of hydrogen in the extremophile *Acidithiobacillus ferrooxidans*. *Frontiers in Microbiology*, 11, 610836. <https://doi.org/10.3389/fmicb.2020.610836>
- Liu, J., Ling, J.-Q., Zhang, K., & Wu, C. D. (2013). Physiological properties of *Streptococcus mutans* UA159 biofilm-detached cells. *FEMS Microbiology Letters*, 340(1), 11–18. <https://doi.org/10.1111/1574-6968.12066>
- Lochman, J., Zapletalova, M., Poskerova, H., Izakovicova Holla, L., & Borilova Linhartova, P. (2019). Rapid multiplex real-time PCR method for the detection and quantification of selected cariogenic and periodontal bacteria. *Diagnostics*, 10(1), 8. <https://doi.org/10.3390/diagnostics10010008>
- Loo, C. Y., Corliss, D. A., & Ganeshkumar, N. (2000). *Streptococcus gordonii* biofilm formation: Identification of genes that code for biofilm phenotypes. *Journal of Bacteriology*, 182(5), 1374–1382. <https://doi.org/10.1128/JB.182.5.1374-1382.2000>

- Love, M. I., Huber, W., & Anders, S. (2014). Moderated estimation of fold change and dispersion for RNA-seq data with DESeq2. *Genome Biology*, 15(12), 550. <https://doi.org/10.1186/s13059-014-0550-8>
- Mattos-Graner, R. O., & Duncan, M. J. (2017). Two-component signal transduction systems in oral bacteria. *Journal of Oral Microbiology*, 9(1), 1400858. <https://doi.org/10.1080/20002297.2017.1400858>
- Merritt, J., & Qi, F. (2012). The mutacins of *Streptococcus mutans*: Regulation and ecology. *Molecular Oral Microbiology*, 27(2), 57–69. <https://doi.org/10.1111/j.2041-1014.2011.00634.x>
- Nomura, R., Nakano, K., & Ooshima, T. (2005). Molecular analysis of the genes involved in the biosynthesis of serotype specific polysaccharide in the novel serotype k strains of *Streptococcus mutans*. *Oral Microbiology and Immunology*, 20(5), 303–309. <https://doi.org/10.1111/j.1399-302X.2005.00231.x>
- Ozaki, K., Shibata, Y., Yamashita, Y., Nakano, Y., Tsuda, H., & Koga, T. (2002). A novel mechanism for glucose side-chain formation in rhamnose-glucose polysaccharide synthesis. *FEBS Letters*, 532(1–2), 159–163. [https://doi.org/10.1016/s0014-5793\(02\)03661-x](https://doi.org/10.1016/s0014-5793(02)03661-x)
- Peng, Y., Kumar, S., Hernandez, R. L., Jones, S. E., Cadle, K. M., Smith, K. P., & Varela, M. F. (2009). Evidence for the transport of maltose by the sucrose permease, CscB, of *Escherichia coli*. *Journal of Membrane Biology*, 228(2), 79–88. <https://doi.org/10.1007/s00232-009-9161-9>
- Pessione, E. (2012). Lactic acid bacteria contribution to gut microbiota complexity: Lights and shadows. *Frontiers in Cellular and Infection Microbiology*, 2, 86. <https://doi.org/10.3389/fcimb.2012.00086>
- Qi, F., Merritt, J., Lux, R., & Shi, W. (2004). Inactivation of the *ciaH* Gene in *Streptococcus mutans* diminishes mutacin production and competence development, alters sucrose-dependent biofilm formation, and reduces stress tolerance. *Infection and Immunity*, 72(8), 4895–4899. <https://doi.org/10.1128/IAI.72.8.4895-4899.2004>
- Ren, Z., Chen, L., Li, J., & Li, Y. (2016). Inhibition of *Streptococcus mutans* polysaccharide synthesis by molecules targeting glycosyltransferase activity. *Journal of Oral Microbiology*, 8, 31095. <https://doi.org/10.3402/jom.v8.31095>
- Rice, K. C., Turner, M. E., Carney, O. V., Gu, T., & Ahn, S.-J. (2017). Modification of the *Streptococcus mutans* transcriptome by LrgAB and environmental stressors. *Microbial Genomics*, 3(2), e000104. <https://doi.org/10.1099/mgen.0.000104>
- Rühmann, B., Schmid, J., & Sieber, V. (2014). Fast carbohydrate analysis via liquid chromatography coupled with ultra violet and electrospray ionization ion trap detection in 96-well format. *Journal of Chromatography A*, 1350, 44–50. <https://doi.org/10.1016/j.chroma.2014.05.014>
- Salminen, S., von Wright, A., & Ouwehand, A. (2004). *Lactic acid bacteria: Microbiological and functional aspects*. Marcel Dekker.
- Sobral, R. G., Jones, A. E., Des Etages, S. G., Dougherty, T. J., Peitzsch, R. M., Gaasterland, T., Ludovice, A. M., de Lencastre, H., & Tomasz, A. (2007). Extensive and genome-wide changes in the transcription profile of *Staphylococcus aureus* induced by modulating the transcription of the cell wall synthesis gene *murF*. *Journal of Bacteriology*, 189(6), 2376–2391. <https://doi.org/10.1128/JB.01439-06>
- Sobral, R. G., Ludovice, A. M., de Lencastre, H., & Tomasz, A. (2006). Role of *murF* in cell wall biosynthesis: Isolation and characterization of a *murF* conditional mutant of *Staphylococcus aureus*. *Journal of Bacteriology*, 188(7), 2543–2553. <https://doi.org/10.1128/JB.188.7.2543-2553.2006>
- Son, M., Ghoreishi, D., Ahn, S.-J., Burne, R. A., & Hagen, S. J. (2015). Sharply tuned pH response of genetic competence regulation in *Streptococcus mutans*: A microfluidic study of the environmental sensitivity of *comX*. *Applied and Environmental Microbiology*, 81(16), 5622–5631. <https://doi.org/10.1128/AEM.01421-15>
- Song, L., Sudhakar, P., Wang, W., Conrads, G., Brock, A., Sun, J., Wagner-Döbler, I., & Zeng, A.-P. (2012). A genome-wide study of two-component signal transduction systems in eight newly sequenced mutans streptococci strains. *BMC Genomics*, 13, 128. <https://doi.org/10.1186/1471-2164-13-128>
- Spatafora, G., Rohrer, K., Barnard, D., & Michalek, S. (1995). A *Streptococcus mutans* mutant that synthesizes elevated levels of intracellular polysaccharide is hypercariogenic in vivo. *Infection and Immunity*, 63(7), 2556–2563. <https://doi.org/10.1128/iai.63.7.2556-2563.1995>
- Staat, R. H., Langley, S. D., & Doyle, R. J. (1980). *Streptococcus mutans* adherence: Presumptive evidence for protein-mediated attachment followed by glucan-dependent cellular accumulation. *Infection and Immunity*, 27(2), 675–681. <https://doi.org/10.1128/iai.27.2.675-681.1980>
- Tanzer, J. M., Thompson, A., Wen, Z. T., & Burne, R. A. (2006). *Streptococcus mutans*: Fructose transport, xylitol resistance, and virulence. *Journal of Dental Research*, 85(4), 369–373. <https://doi.org/10.1177/154405910608500417>
- Trahan, L., Néron, S., & Bareil, M. (1991). Intracellular xylitol-phosphate hydrolysis and efflux of xylitol in *Streptococcus sobrinus*. *Oral Microbiology and Immunology*, 6(1), 41–50. <https://doi.org/10.1111/j.1399-302x.1991.tb00450.x>
- van der Beek, S. L., Zorzoli, A., Çanak, E., Chapman, R. N., Lucas, K., Meyer, B. H., Evangelopoulos, D., de Carvalho, L. P. S., Boons, G.-J., Dorfmüller, H. C., & van Sorge, N. M. (2019). Streptococcal dTDP-L-rhamnose biosynthesis enzymes: Functional characterization and lead compound identification. *Molecular Microbiology*, 111(4), 951–964. <https://doi.org/10.1111/mmi.14197>
- van der Ploeg, J. R. (2005). Regulation of bacteriocin production in *Streptococcus mutans* by the quorum-sensing system required for development of genetic competence. *Journal of Bacteriology*, 187(12), 3980–3989. <https://doi.org/10.1128/JB.187.12.3980-3989.2005>
- Welin, J., Wilkins, J. C., Beighton, D., Wrzesinski, K., Fey, S. J., Mose-Larsen, P., Hamilton, I. R., & Svensäter, G. (2003). Effect of acid shock on protein expression by biofilm cells of *Streptococcus mutans*. *FEMS Microbiology Letters*, 227(2), 287–293. [https://doi.org/10.1016/S0378-1097\(03\)00693-1](https://doi.org/10.1016/S0378-1097(03)00693-1)
- Wen, Z. T., Jorgensen, A. N., Huang, X., Ellepola, K., Chapman, L., Wu, H., & Brady, L. J. (2021). Multiple factors are involved in regulation of extracellular membrane vesicle biogenesis in *Streptococcus mutans*. *Molecular Oral Microbiology*, 36(1), 12–24. <https://doi.org/10.1111/omi.12318>
- Willenborg, J., & Goethe, R. (2016). Metabolic traits of pathogenic streptococci. *FEBS Letters*, 590(21), 3905–3919. <https://doi.org/10.1002/1873-3468.12317>
- Wilson, W. A., Roach, P. J., Montero, M., Baroja-Fernández, E., Muñoz, F. J., Eydallin, G., Viale, A. M., & Pozueta-Romero, J. (2010). Regulation of glycogen metabolism in yeast and bacteria. *FEMS Microbiology Reviews*, 34(6), 952–985. <https://doi.org/10.1111/j.1574-6976.2010.00220.x>
- Zeng, L., & Burne, R. A. (2008). Multiple sugar: Phosphotransferase system permeases participate in catabolite modification of gene expression in *Streptococcus mutans*. *Molecular Microbiology*, 70(1), 197–208. <https://doi.org/10.1111/j.1365-2958.2008.06403.x>
- Zeng, L., & Burne, R. A. (2013). Comprehensive mutational analysis of sucrose-metabolizing pathways in *Streptococcus mutans* reveals novel roles for the sucrose phosphotransferase system permease. *Journal of Bacteriology*, 195(4), 833–843. <https://doi.org/10.1128/JB.02042-12>
- Zeng, L., & Burne, R. A. (2016). Sucrose- and fructose-specific effects on the transcriptome of *Streptococcus mutans*, as determined by RNA sequencing. *Applied and Environmental Microbiology*, 82(1), 146–156. <https://doi.org/10.1128/AEM.02681-15>
- Zeng, L., Das, S., & Burne, R. A. (2010). Utilization of lactose and galactose by *Streptococcus mutans*: Transport, toxicity, and carbon catabolite repression. *Journal of Bacteriology*, 192(9), 2434–2444. <https://doi.org/10.1128/JB.01624-09>
- Zeng, L., Das, S., & Burne, R. A. (2011). Genetic analysis of the functions and interactions of components of the LevQRST signal transduction complex of *Streptococcus mutans*. *PLoS ONE*, 6(2), e17335. <https://doi.org/10.1371/journal.pone.0017335>

Zhang, T., Zhu, J., Xu, J., Shao, H., & Zhou, R. (2020). Regulation of (p)ppGpp and its homologs on environmental adaptation, survival, and pathogenicity of streptococci. *Frontiers in Microbiology*, *11*, 1842. <https://doi.org/10.3389/fmicb.2020.01842>

SUPPORTING INFORMATION

Additional supporting information can be found online in the Supporting Information section at the end of this article.

How to cite this article: Jurakova, V., Farková, V., Kucera, J., Dadakova, K., Zapletalova, M., Paskova, K., Reminek, R., Glatz, Z., Holla, L. I., Ruzicka, F., Lochman, J., & Linhartova, P. B. (2023). Gene expression and metabolic activity of *Streptococcus mutans* during exposure to dietary carbohydrates glucose, sucrose, lactose, and xylitol. *Molecular Oral Microbiology*, *38*, 424–441. <https://doi.org/10.1111/omi.12428>